Applied Energy 416 (2026) 127973

Contents lists available at ScienceDirect

Applied Energy

journal homepage: www.elsevier.com/locate/apen

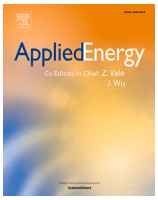

A framework for flexibility assessment of district heating and cooling systems

Leopold Riedl [a,*], Sebastian Zwickl-Bernhard [a,b], Lukas Kranzl [a], Hanne Kauko [c], Christopher Schifflechner [d]

[a] Energy Economics Group (EEG), Technische Universität Wien, Gusshausstrasse 25-29/E370-3, 1040 Wien, Austria
[b] Department of Industrial Economics and Technology Management, The Norwegian University of Science and Technology, Trondheim, Norway
[c] SINTEF Energy Research, Postboks 4761 Torgarden, Trondheim, NO-7465, Norway
[d] Chair of Energy Systems, Technical University of Munich, Boltzmannstr. 15, 85748 Garching, Germany

HIGHLIGHTS

- A transferable framework for assessing district heating and cooling flexibility.
- Integrated approach links flexibility with techno-economic performance metrics.
- Framework applied to a developing district heating and cooling system in Trondheim.
- Heating subsystems dominate flexibility provision; cooling contributes negligibly.
- Flexibility indicators remain robust across policy and climate scenario variations.

ARTICLE INFO

Keywords:
District heating and cooling
Flexibility assessment
Performance indicators
Demand-side flexibility
Sector coupling

ABSTRACT

District heating and cooling (DHC) systems represent significant flexibility resources for electricity grids, yet systematic assessment and comparison of their flexibility potential are hindered by the absence of a consistent quantitative framework. This study introduces a comprehensive key performance indicator framework that integrates demand-side flexibility metrics with storage dynamics and system performance indicators to enable systematic evaluation and benchmarking of DHC flexibility provision. Applying the framework to a Norwegian case study across diverse scenarios demonstrates its ability to reveal heating-dominated flexibility patterns and assess the robustness of indicators under varying policy and climate conditions. The framework shifts the evaluation paradigm from traditional thermal output metrics to systematic flexibility assessment, enabling decision-makers to quantify not only whether DHC systems provide flexibility, but how much, under what constraints, and at what cost. This establishes a methodological foundation for comparing different configurations and developing flexibility-oriented approaches in DHC planning.

1. Introduction

The large-scale integration of variable renewable energy sources (VRES), such as solar and wind, increases volatility in electricity markets [1,2]. These price fluctuations incentivize energy actors to unlock the flexibility potential across vectors, such as gas and thermal energy, through price arbitrage [3].

District heating and cooling (DHC) systems are well-positioned to provide flexibility to the power grid. Their increasing electrification through power-to-heat technologies, such as heat pumps (HPs) and electric boilers, enables them to adjust their electricity consumption in response to price variations, thereby supporting system balancing and market integration [4]. However, the actual provision of flexibility from DHC networks remains limited compared to their technical potential [5]. Several factors contribute to this discrepancy, including operational priorities that focus on ensuring heat supply security, limited economic incentives for flexibility, and institutional settings that do not yet fully recognize DHC as an active player in energy markets [6,7].

* Corresponding author.
Email address: riedl@eeg.tuwien.ac.at (L. Riedl).

https://doi.org/10.1016/j.apenergy.2026.127973
Received 6 February 2026; Received in revised form 10 April 2026; Accepted 21 April 2026
Available online 2 May 2026

One underlying reason for the limited utilization of DHC flexibility lies in the traditional view of DHC systems. Unlike the gas and electricity sectors, DHC has not undergone European-wide market standardization or liberalization. Consequently, DHC systems operate in largely unregulated environments with limited market oversight, where prices tend to be less transparent and more susceptible to abuses of market power [8]. These structural characteristics hinder the integration of DHCs into competitive energy markets and thereby limit their contribution to overall system flexibility. Previous studies also underline a considerable gap between the potential and actual flexibility contributions of DHC systems. Especially relevant for our case study, Kauko et al. [9] analyzed the entire Norwegian building stock and demonstrated that large-scale deployment of district heating with heat pumps, combined with high efficiency standards, could reduce total electricity demand by 26% and peak electricity demand by 35%, highlighting untapped opportunities.

One of the main reasons for this unused potential is the lack of a clear understanding of what kind of flexibility DHC systems can actually provide to the power system [10]. While existing research has focused on technical modeling [11–13] or case-specific simulations [14–16], a consistent methodology to quantify, compare, and benchmark DHC flexibility across different contexts is lacking. This knowledge gap limits scientific understanding and creates uncertainty for DHC operators, energy actors and regulators when assessing the role of DHC in future integrated multi-energy systems.

To address these gaps, we investigate the following research questions:

1. How can a quantitative framework be designed to systematically assess and compare the flexibility potential of DHC systems?
2. What flexibility potential does the framework reveal for DHC systems across temporal horizons and varying scenarios, and which system characteristics prove robust versus sensitive to external conditions?

This study aims to enhance understanding of the flexibility potential and provision of DHC systems by introducing a quantitative key performance indicator (KPI) framework to support decision-making in integrated multi-energy systems. We apply the framework to a Norwegian case study (Trondheim, 2025–2040), quantifying flexibility potential across scenarios and comparing results to benchmarks from existing studies. While the case study provides an empirical illustration, the primary contribution is the transferable methodology for systematic flexibility assessment and comparison of DHC configurations under varying external conditions. The selected indicators are intended to inform both operational assessment and planning oriented evaluation of flexibility provision. This introduces a new dimension of flexibility assessment into the broader discussion on electricity grid integration and energy system planning.

2. Relevant literature

The performance assessment of DHC systems has changed from narrow technical evaluations to comprehensive, multi-dimensional frameworks, reflecting the growing complexity of energy system integration. Earlier studies primarily focused on thermodynamic performance, evaluating DHC systems in terms of energy and exergy efficiency [17], primary energy factors and savings [18], or a combination of these metrics for specific applications such as biomass-based systems [19]. More recent frameworks adopt multi-dimensional approaches, combining economic, environmental, and operational indicators to provide a more comprehensive evaluation. For instance, Ivancic et al. [20] propose a framework of eleven KPIs covering resource efficiency, environmental impact, and social aspects, while Millar et al. [21] and Gjoka et al. [22] assess fifth-generation DHC systems using metrics such as levelized costs, self-sufficiency rates, and life-cycle emissions. Similarly, Zhang et al. [23] compare different DHC configurations from technical, economic, and environmental perspectives, explicitly accounting for future uncertainties. While these studies provide valuable insights into system performance, quantifiable flexibility metrics remain largely absent from existing assessment frameworks. Notable exceptions include Guelpa and Verda [24], who review thermal energy storage (TES) in DHC systems and its role in flexibility provision, and Du et al. [25], who incorporate two flexibility-related KPIs into their assessment of district heating systems integrated with data centers. However, a systematic framework for evaluating the flexibility potential of DHC systems has yet to be developed.

In parallel, a substantial body of literature has emerged on flexibility assessment in energy systems more broadly. Early studies emphasized the necessity of flexibility in systems with increasing shares of VRES, examining technical potentials, economic incentives, and market-based mechanisms [26,27]. Subsequent work has sought to establish comprehensive definitions and taxonomies for flexibility resources [28,29], with recent contributions proposing multi-dimensional characterizations that consider time, space, resource type, and risk [30]. Several studies at the power system level have developed metrics for integrating flexibility considerations into generation planning [31,32], while others have proposed indicator frameworks for comparing flexibility across different countries or systems [33,34]. A consistent finding across these studies is the absence of a unified definition of flexibility and the requirement for standardized quantification methods that are transferable across diverse energy system contexts.

Within the broader field of building energy flexibility, most studies focus on the building scale [35,36], examining load shifting, demand response, and the flexibility potential of thermal mass and thermal energy storage (TES) systems [37]. Several authors have proposed quantification methods based on power, energy, and time dimensions [38–40], while others have developed dynamic approaches that characterize flexibility as a time-varying property rather than a static value [41]. Recent contributions have also emphasized the need for standardized procedures and baseline-free indicators derived from real-time performance data [42]. While most studies employ deterministic approaches, Yuan et al. [43] address uncertainties related to building characteristics and occupant behavior, although their analysis remains limited to electric power flexibility. More recent contributions have begun to address the aggregation of building flexibility at larger scales, proposing frameworks for building clusters [44], microgrids [45], or multi-energy systems [46,47]. These approaches are important steps towards assessing system-level flexibility, introducing concepts such as resource-independent quantification and distinguishing between direct and indirect metrics that capture economic or environmental impacts. However, they have primarily been developed for individual buildings or electricity-centric systems, rather than for integrated DHC systems.

Recent research on DHC flexibility has systematically explored the sources and mechanisms through which these systems can provide flexibility services. Research on the supply side has primarily focused on integrating the electricity and heating sectors through power-to-heat technologies [48] and combined heat and power plants. In this context, flexibility is defined as the period during which the operation of a plant can be varied [49]. On the demand side, DH systems can leverage TES, the water mass within network pipelines, and the thermal inertia of connected buildings to decouple heat supply from demand [50–52]. In an earlier work [10] provides an overview of heating flexibility sources within buildings and potential quantification methods, while subsequent studies demonstrate the significant load shifting potential of building envelope thermal inertia [53]. The benefits of such demand-side management strategies are well documented, including peak shaving, reduced emissions, and increased load factors [50]. While several authors have proposed indicators based on power, energy, and ramping ability [48], and others have examined how DH flexibility can be integrated into electricity markets [5], a systematic quantification of flexibility potential remains elusive. Moreover, studies that incorporate stakeholder perspectives reveal that the absence of economic incentives and inadequate regulatory frameworks pose significant challenges to

Table 1
Summary of identified research gaps and contributions of this study.

Research stream	Focus	Key metrics	Identified gap	Contribution of this study
DHC performance	Multi-dimensional assessment (thermodynamic, economic, environmental)	Levelized costs, exergy efficiency, primary energy factors	Flexibility metrics largely absent; where present, fragmented rather than systematic	Systematic integration of flexibility indicators into holistic DHC assessment
General energy flexibility	Power systems, buildings, and multi-energy systems	Load shifting, demand response, flexibility indices	Electricity-centric; lacks standardized methods transferable to DHC contexts	Flexibility metrics tailored to thermal sector coupling in electrified DHC systems
DHC-specific flexibility	Supply and demand side mechanisms (TES, inertia, network)	Power, energy, and ramping indicators	Sources identified but no standardized quantification for cross-system comparison	A framework with context-adaptable thresholds that enables cross-system comparability

realizing this potential in practice, as noted by Ma et al. [6] and Fernqvist et al. [54].

Table 1 synthesizes the identified research gaps across these three research streams and highlights the specific contributions and novelty of this study.

As outlined in Table 1, the existing literature reveals a fundamental disconnect between three research streams. DHC performance assessments have evolved into multidimensional frameworks but neglect flexibility metrics essential for grid interaction. Flexibility assessments in energy systems are methodologically robust but remain focused on electricity-centric or building-level analyses, overlooking DHC-specific contributions. DHC-specific flexibility studies identify key sources and mechanisms but lack standardized quantification methods for comparative assessment across systems. Building on these identified gaps, this study introduces the following three novel contributions:

- A comprehensive assessment framework is developed that systematically integrates demand-side flexibility indicators with traditional performance metrics (thermodynamic, economic and environmental). This enables a multi-dimensional evaluation of DHC systems that explicitly accounts for their role in grid interaction.
- Methods for quantifying flexibility from the broader energy systems literature are extended and adapted to capture the specific characteristics of electrified DHC systems, including thermal storage dynamics and price-responsive operation as indicators of sector coupling.
- A systematic benchmarking structure with context-adaptable thresholds is introduced. This allows for standardized comparisons of flexibility provision across different DHC configurations and scenarios.

3. Method

This section presents the modeling approach used to assess the flexibility potential of DHC systems. The main idea of this study is to combine energy system modeling with a newly developed KPI framework to quantify how DHC systems can provide flexibility to the power system. Fig. 1 provides an overview of the proposed methodology, comprising three components: the data foundation, the KPI framework with its flexibility and system performance indicators, and the comparative assessment approach. The focus of this section lies on the novel aspects of this study, particularly the composition and application of the KPI framework, rather than the mathematical details of the underlying optimization models. Therefore, a detailed explanation of how each KPI is calculated and interpreted is provided, as these indicators represent the core innovation of this paper. In contrast, the description of the supporting models is kept concise, limiting it to aspects directly relevant to generating the input data required by the KPI framework. Readers seeking deeper insights into the mathematical formulations of the models should refer to the relevant literature and documentation cited in the subsequent sections describing the respective models.

The section is structured as follows: Section 3.1 introduces the KPI framework, starting with a brief description of the input-output relations of the underlying stochastic optimization model, whose results serve as the basis for generating the KPIs. This is followed by detailed descriptions of the individual KPIs, including their calculation and main implications. Finally, Section 3.2 provides an overview of the models used to apply the framework, as well as the case study examined.

3.1. KPI framework

The proposed framework is intended for grid-coupled, electrified DHC systems where electricity consumption can be modulated in response to grid conditions. It enables systematic assessment of whether and to what extent such systems can provide flexibility services to the electricity grid. Its primary focus lies on operational flexibility, capturing aspects such as the system's response to price signals and utilization of available capacities for load adjustment. Investment decisions are captured indirectly, as the installed technology portfolio influences both the operational flexibility available and the economic and environmental performance of the system.

The framework comprises indicators that are either already established in the literature or derived from it, as well as newly developed metrics. Each indicator is introduced with a clear explanation of its calculation method, the required input data, and its relevance to assessing flexibility provision or overall system efficiency. To ensure a comprehensive and targeted analysis, the framework distinguishes between two groups of indicators. The first group focuses specifically on flexibility aspects, capturing various dimensions of operational adaptability, such as the system's ability to adjust its electricity consumption based on external price signals or the use of TES capacities. The second category includes broader performance indicators that extend the analysis to economic and environmental aspects, such as the levelized cost of heating and cooling and CO_2 emissions. This dual structure enables both a detailed evaluation of flexibility potential and a comprehensive assessment of the system's overall performance.

Flexibility indicators focus on electricity-thermal sector coupling, making them most relevant for systems with substantial power-to-heat technologies. DHC systems relying on non-electric sources (e.g., deep geothermal) may score unfavorably on flexibility metrics despite providing grid-independent stability. These systems should therefore be evaluated using frameworks emphasizing thermal reliability.

3.1.1. Input-output relations

The district energy stochastic portfolio optimization model (DESPO), described in Section 3.2.2, integrates demand profiles for heating and cooling, various cost parameters for investment, operations and maintenance, and market-driven electricity and gas prices, as well as environmental factors such as solar radiation and temperature. It employs stochastic optimization to account for uncertainties in areas such as energy prices, demand patterns, policy measures, and other relevant parameters.

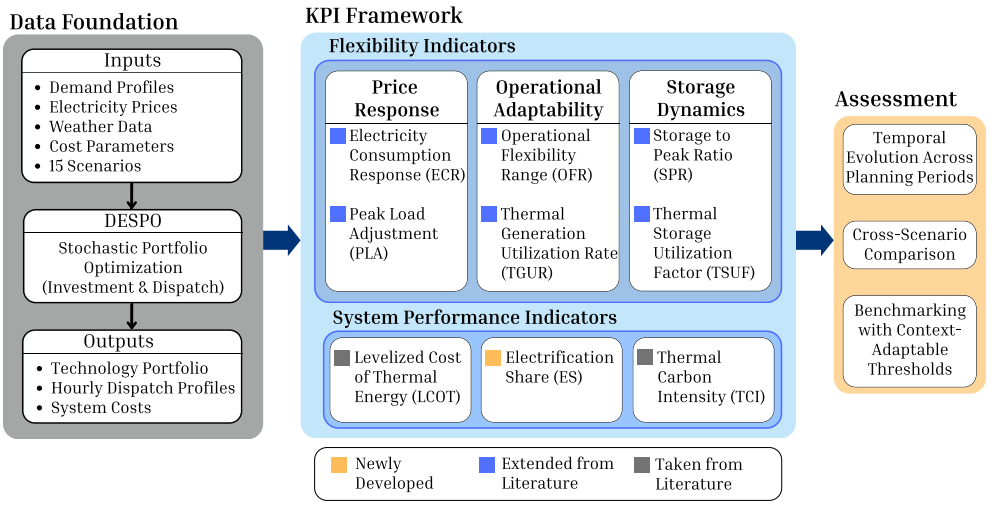

Fig. 1. Overview of the methodological approach.

The outputs of DESPO – optimal technology capacities (scenario-independent), hourly operational data (scenario-dependent), and associated system costs – form the quantitative basis of the KPI framework.

3.1.2. Flexibility KPIs

The flexibility indicators are selected to enable consistent assessment of demand-side flexibility in electrified DHC systems. They address key questions such as how the system responds to electricity price signals, what operational flexibility is available within technical constraints, to what extent TES enables temporal load shifting and how effectively this potential is utilized. These questions correspond to three complementary flexibility dimensions, namely price response, operational adaptability, and storage dynamics.

Indicator selection follows four criteria: the KPIs are (i) derivable from widely available operational time series and basic system characteristics (from either optimization outputs or measured system data), (ii) interpretable with a clear physical or economic meaning and a defined direction of improvement, (iii) non-redundant, capturing distinct flexibility dimensions rather than overlapping information, and (iv) robust through paired metrics within each dimension that enable cross-validation and reduce the risk of misleading conclusions from any single indicator. To maximize transferability across electrified DHC applications, the selection deliberately relies on data- and context-agnostic metrics, avoiding indicators that depend on detailed electricity grid constraints or specific market product definitions. Alternative indicators such as ramp rates or response times were considered but excluded because they primarily characterize sub-hourly dynamics beyond the temporal resolution of the underlying optimization model.

Electricity Consumption Response (ECR): This indicator is adapted from demand response metrics that quantify changes in energy consumption between peak and off-peak operating conditions [55]. It measures the relative change in total annual electricity consumption of the DHC system under variable electricity prices compared to a constant price baseline. The metric is derived by comparing two optimization runs for each scenario: one with time-varying electricity prices reflecting real market conditions, and one with a constant price set to the annual average. The relative difference in total annual electricity consumption between these runs reveals the system's net electricity consumption response to price signals. The ECR for year y and scenario s is calculated using Eq. (1).

$$ECR_{y,s}^{con,elec} = \frac{\sum_{h \in H} (q_{y,s,h}^{con,elec,var} - q_{y,s,h}^{con,elec,const})}{\sum_{h \in H} q_{y,s,h}^{con,elec,const}} \times 100\% \quad : \forall\, y, s \tag{1}$$

In this equation, $q_{y,s,h}^{con,elec,var}$ represents the hourly electricity consumption under variable prices for year y, scenario s, and hour $h \in H$. The term $q_{y,s,h}^{con,elec,const}$ denotes the corresponding consumption under constant prices for the same conditions. The set $H = \{1, 2, \ldots, 8760\}$ indexes all hours of the year.

A positive ECR indicates that the system consumes more electricity under variable prices than under the constant price baseline over the year, for example by increasing the operation of electricity-dependent technologies during low price periods. Conversely, a negative ECR indicates a net reduction in annual electricity consumption under variable prices, for instance through switching to non-electric supply options during high price periods. Importantly, ECR reflects the net annual energy volume effect, rather than the temporal redistribution of electricity consumption within the year. Therefore, even when substantial load shifting occurs, the ECR may remain close to zero if periods of increased and decreased electricity use offset each other over time. For this reason, ECR is interpreted alongside indicators that capture operational adaptability and storage utilization. Together, these indicators provide a more complete picture of flexibility provision. By design, the ECR is an energy-based metric that quantifies the net change in electricity consumption in response to price signals. It does not account for the magnitude of price variations themselves, meaning consumption shifts during high- and low-price periods are treated equally in terms of energy volume. However, a price-weighted extension of the ECR, such as integrating price differentials into the metric, could differentiate scenarios based on the economic significance of consumption shifts, offering a more nuanced perspective on the interplay between energy and price dynamics. This refinement is proposed as future work.

Peak Load Adjustment (PLA): Adapted from demand response quantification methods that estimate load reduction potential through setpoint adjustments relative to baseline consumption [56], this indicator evaluates how the system's peak electricity demand varies between variable and constant price conditions. It highlights the system's ability to adapt its maximum load in response to price signals, which is particularly relevant for grid stability and demand-side management. The PLA for year y and scenario s is calculated as:

$$PLA_{y,s}^{peak,elec} = \frac{q_{y,s}^{peak,elec,var} - q_{y,s}^{peak,elec,const}}{q_{y,s}^{peak,elec,const}} \times 100\% \quad : \forall\, y, s \tag{2}$$

where $q_{y,s}^{peak,elec,var}$ is the peak electricity demand (in MW) observed under variable prices for year y and scenario s, while $q_{y,s}^{peak,elec,const}$ denotes the peak demand under constant prices for the same conditions.

A negative PLA signals peak shaving, where the system reduces maximum electricity demand by deploying alternative supply technologies or TES during peak periods. A positive PLA suggests a peak shift or slight increase due to optimized dispatch. This capability mitigates peak price exposure and grid congestion, enhancing system resilience during critical demand phases.

It is important to note that this metric focuses on the magnitude of peak demand rather than its timing. It compares maximum electricity demand across the entire year under different price conditions, which may occur at different hours. A PLA of 0% shows the peak remains unchanged, but the system may still provide peak-shaving services during high-price periods, while experiencing maximum load at a different time, such as during thermal demand peaks that do not coincide with price peaks.

Operational Flexibility Range (OFR): The OFR is adapted from the convex hull approach introduced by Zwickl-Bernhard et al. [57], who visualize operational flexibility using absolute electricity consumption and thermal supply values. This indicator extends the method by normalizing both dimensions relative to cumulative installed capacity to enable comparison across planning periods with different technology portfolios. For each scenario and year, the total electricity consumption of all electricity-dependent technologies $t \in \mathcal{T}^{elec}$ (e.g., heat pumps, electric chillers) is plotted against their thermal (heat or cool) energy supply. Only electricity-dependent technologies are considered, as their operation directly influences the system's flexibility in response to electricity price signals. The resulting scatter plots, created separately for heating and cooling, comprise 60 data points (15 scenarios and 4 years) and illustrate the system's adaptive operation under varying conditions between scenarios. To enable fair comparison across years with different installed capacities, both electricity consumption and thermal supply are normalized relative to the cumulative capacity installed up to each respective year. The normalized electricity consumption for year y and scenario s is given by Eq. (3):

$$q^{elec,norm}_{y,s} = \frac{\sum_{t\in\mathcal{T}^{elec}} q^{con,elec}_{y,s,t}}{\sum_{y'\le y}\sum_{t\in\mathcal{T}^{elec}} p^{cap,elec}_{y',t}\times 8760} \quad \forall\, y,s \tag{3}$$

where $\sum_{t\in\mathcal{T}^{elec}} q^{con,elec}_{y,s,t}$ represents the annual electricity consumption (in MWh) of all electricity-dependent technologies in year y and scenario s. The denominator aggregates the cumulative installed electrical capacity (in MW) of these technologies up to and including year y, multiplied by 8760 hours to convert it to energy units.

Similarly, the normalized thermal supply is defined in Eq. (4):

$$q^{th,norm}_{y,s} = \frac{\sum_{t\in\mathcal{T}^{elec}} q^{sup,th}_{y,s,t}}{\sum_{y'\le y}\sum_{t\in\mathcal{T}^{elec}} p^{cap,th}_{y',t}\times 8760} \quad \forall\, y,s \tag{4}$$

Here, $\sum_{t\in\mathcal{T}^{elec}} q^{sup,th}_{y,s,t}$ describes the annual thermal (heat or cooling) supply of all electricity-dependent technologies t in year y and scenario s. The denominator reflects the cumulative installed thermal capacity (in MW) up to year y.

These normalized values are plotted and the convex hull of all data points is calculated, which defines the operational flexibility envelope. The area of this polygon serves as the quantitative metric for operational flexibility:

$$OFR = \text{Area}\left(\text{ConvexHull}\left\{\left(q^{th,norm}_{y,s}, q^{elec,norm}_{y,s}\right) \mid \forall\, y,s\right\}\right) \tag{5}$$

A larger OFR value indicates greater operational flexibility, as the system demonstrates a wider range of electricity consumption levels for given thermal outputs across different scenarios. This reflects the system's ability to adjust technology dispatch in response to varying conditions. The OFR is dimensionless and ranges from 0 to 1, where higher values indicate more diverse operational strategies available to the system.

Thermal Generation Utilization Rate (TGUR): This indicator is adapted from capacity utilization metrics that assess the effective use of individual components such as heat pumps and storage tanks [58]. It evaluates the intensity with which electrical thermal generation technologies are utilized. It compares the actual annual thermal output with the theoretical maximum if all technologies operated at full capacity throughout the year. The TGUR for year y and scenario s is defined in Eq. (6):

$$TGUR_{y,s} = \frac{\sum_{t\in\mathcal{T}^{elec}} q^{sup,th}_{y,s,t}}{\sum_{y'\le y}\sum_{t\in\mathcal{T}^{elec}} p^{cap,th}_{y',t}\times 8760} \times 100\% \quad : \forall\, y,s \tag{6}$$

where, $\sum_{t\in\mathcal{T}^{elec}} q^{sup,th}_{y,s,t}$ represents the annual thermal output (in MWh) from all electricity-dependent generation technologies t in year y and scenario s. The denominator reflects the cumulative installed thermal capacity (in MW) up to and including year y, multiplied by 8760 hours to represent the theoretical maximum annual output.

The resulting utilization rate provides critical insights into the system's operational behavior. A high utilization rate approaching 100% indicates that technologies operate near maximum capacity for most of the year, characteristic of baseload operation with limited flexibility. Conversely, a low utilization rate suggests that substantial installed capacity remains underutilized, indicating greater potential for upward flexibility.

Storage to Peak Ratio (SPR): This indicator is adapted from metrics relating to the reduction in peak demand through thermal storage capacity [59], and expresses the relationship between installed thermal energy storage (TES) capacity and the system's peak thermal demand. It represents the theoretical number of hours that fully charged storage could supply the maximum hourly demand. By quantifying this relationship, the SPR provides insight into the system's capacity for temporal load shifting during critical demand periods. The SPR for year y and scenario s is calculated as:

$$SPR_{y,s} = \frac{\sum_{y'\le y}\sum_{t\in\mathcal{T}^{sto}} q^{cap,sto}_{y',t}}{\max_{h\in H}\sum_{t} q^{sup,th}_{y,s,h,t}} \quad \forall\, y,s \tag{7}$$

where $\sum_{y'\le y}\sum_{t\in\mathcal{T}^{sto}} q^{cap,sto}_{y',t}$ represents the cumulative installed storage energy capacity (in MWh) across all storage technologies up to and including year y. The denominator identifies the peak hourly thermal demand (in MW), defined as the maximum thermal supply across all hours h in year y and scenario s.

The resulting ratio indicates how many hours of peak demand the TES could theoretically cover if fully charged. A higher SPR indicates substantial buffering capacity for managing demand peaks and price volatility, while a lower value suggests that storage plays a limited role in short-term demand balancing. This metric is particularly relevant for assessing the system's ability to decouple thermal supply from electricity consumption during periods of high electricity prices or grid constraints.

Thermal Storage Utilization Factor (TSUF): This indicator is newly proposed in this study to quantify how actively TES systems are utilized by measuring the total charging and discharging activity relative to the maximum possible throughput. Storage activity is determined by summing the absolute changes in the state of charge between consecutive hours across all storage technologies throughout the year. This value is then normalized by the theoretical maximum throughput, which represents the total energy that could flow through the storage if it operated at full capacity in both directions for every hour. The TSUF is expressed as shown in Eq. (8):

$$TSUF_{y,s} = \frac{\sum_{t\in\mathcal{T}^{sto}}\sum_{h\in H}\left|q^{sto}_{y,s,h,t} - q^{sto}_{y,s,h-1,t}\right|}{2\times\sum_{t\in\mathcal{T}^{sto}}\left(\sum_{y'\le y} p^{cap,th}_{y',t}\right)\times 8760} \times 100\% \quad \forall\, y,s \tag{8}$$

where $q^{sto}_{y,s,h,t}$ represents the state of charge (in MWh) of storage technology t at hour h in year y and scenario s. The numerator sums the absolute changes in the state of charge between consecutive hours across all storage technologies and all hours $h \in H$. The denominator represents the maximum possible throughput, calculated as twice the cumulative installed charging and discharging power capacity (in MW) up to year y, multiplied by 8760 hours. The factor of 2 accounts for the bidirectional nature of storage, as each unit of capacity can contribute to both charging and discharging.

A high TSUF value indicates frequent and substantial energy shifting, demonstrating intensive use of the storage capacity for load balancing and operational flexibility. Conversely, a low value suggests that the available storage capacity remains largely idle, indicating untapped flexibility potential. This metric therefore reveals how effectively the storage infrastructure contributes to the system's operational flexibility.

3.1.3. System performance and sustainability indicators

To ensure a holistic assessment of DHC systems, flexibility metrics are complemented with performance and sustainability indicators that evaluate economic viability, environmental impact, and operational efficiency. These metrics serve two key purposes:

First, they enable comparative analysis of system configurations, revealing the trade-offs between flexibility, cost-effectiveness, and sustainability. This perspective is crucial for stakeholders because it shows how investments in flexibility, such as storage or electrification, affect long-term economic and environmental outcomes. For example, flexibility-optimized systems can reduce costs through demand response or emissions via renewable integration, whereas cost-driven designs may compromise adaptability.

Second, these indicators provide a context for flexibility by highlighting the synergies and conflicts between technical, economic and environmental performance. High electrification, for instance, increases flexibility but can lead to higher emissions unless it is coupled with renewable energy sources. This analysis provides a balanced framework for decision-making, aligning DHC systems with climate goals, economic constraints, and grid stability.

Levelized Cost of Thermal Energy (LCOT): Following the established LCOH methodology [60], this indicator evaluates the long-term economic viability of the DHC system by calculating the average cost per unit of thermal (heating or cooling) energy supplied over the entire planning horizon from 2025 to 2040. The metric follows the established LCOH methodology but extends it to cover both heating and cooling, hence the term Levelized Cost of Thermal Energy. The LCOT accounts for all discounted costs, including capital investment, fixed operation and maintenance, and variable operational costs such as electricity and fuel expenses. By discounting both costs and energy output, this metric enables fair comparison across different scenarios and technological configurations. The LCOT for scenario s is calculated as follows:

$$LCOT_s = \frac{\sum_y \sum_t \left[\left(c^{inv}_{y,t} + c^{fix}_{y,t} + \sum_{h \in H} c^{var}_{y,s,t,h} \right) \times DF_y \right]}{\sum_y \sum_t \sum_{h \in H} q^{sup,th}_{y,s,t,h} \times DF_y} \quad \forall\, s \tag{9}$$

where the discount factor DF_y for every year y is defined as:

$$DF_y = \frac{1}{(1+r)^{y-2025}} \tag{10}$$

In the numerator, $c^{inv}_{y,t}$ represents the investment costs (in €) for technology t in year y, $c^{fix}_{y,t}$ denotes the annual fixed operation and maintenance costs, and $c^{var}_{y,s,t,h}$ captures the hourly variable operational costs for scenario s. The denominator aggregates the total thermal energy supply $q^{sup,th}_{y,s,t,h}$ (in MWh_{th}) across all technologies, years, and hours. Both the numerator and the denominator are discounted using the discount factor DF_y, which depends on the discount rate r.

The resulting LCOT value, expressed in €/MWh_{th}, represents the average lifetime cost per unit of thermal energy supplied, accounting for all discounted capital, fixed, and variable costs. This standardized metric facilitates the economic evaluation of the DHC system and enables benchmarking against alternative configurations or competing energy supply solutions.

Electrification Share (ES): Newly proposed in this study, this indicator quantifies the degree of electrification in the thermal supply measuring the share of heat and cooling provided by electricity dependent technologies relative to the total thermal energy supply. The ES for year y and scenario s is given by Eq. (11).

$$ES_{y,s} = \frac{\sum_{t \in \mathcal{T}^{elec}} q^{sup,th}_{y,s,t}}{\sum_{t \in \mathcal{T}} q^{sup,th}_{y,s,t}} \times 100\% \quad \forall\, y, s \tag{11}$$

Here, $\sum_{t \in \mathcal{T}^{elec}} q^{sup,th}_{y,s,t}$ represents the annual thermal energy supply (in MWh) from all electricity-dependent technologies t in year y and scenario s. The denominator $\sum_{t \in \mathcal{T}} q^{sup,th}_{y,s,t}$ captures the total annual thermal energy supply from all technologies, including both electric and non-electric options such as gas boilers or waste heat recovery.

A high ES value indicates strong reliance on electricity for thermal supply, which enhances the system's ability to provide flexibility services to the electricity grid and facilitates integration of renewable electricity sources. Conversely, a low share suggests greater dependence on non-electric technologies, which limits the system's responsiveness to electricity price signals but may offer advantages in terms of fuel diversification. This metric is particularly relevant for evaluating the system's potential for sector coupling and its alignment with decarbonization strategies that prioritize electrification of heating and cooling.

Thermal Carbon Intensity (TCI): Based on the established carbon intensity metric used in DHC benchmarking [20], this indicator relates the system's total carbon emissions to the thermal energy supplied to assess the environmental impact of the DHC system. This metric quantifies the emissions per unit of thermal energy, expressed in kg CO_2/MWh_{th}, and can be evaluated separately for heating and cooling or as a combined value for the entire system. By normalizing emissions relative to the energy service provided, the TCI enables fair comparisons across systems of varying sizes and configurations, while highlighting their environmental performance. The TCI for year y and scenario s is derived from the following relationship.

$$TCI_{y,s} = \frac{\sum_t \sum_{h \in H} q^{sup,th}_{y,s,t,h} \times EF_t}{\sum_t \sum_{h \in H} q^{sup,th}_{y,s,t,h}} \quad \forall\, y, s \tag{12}$$

Here, $q^{sup,th}_{y,s,t,h}$ represents the hourly thermal energy supply (in MWh_{th}) from technology t in year y, scenario s, and hour h. Each technology has an associated emission factor EF_t (in kg CO_2/MWh_{th}) that reflects the carbon intensity of its energy source. For electricity-dependent technologies, this factor corresponds to the grid emission factor, while for combustion-based technologies it reflects the fuel-specific emissions (see Appendix A.2, Table 13).

The resulting TCI value provides a direct measure of the system's carbon footprint relative to its thermal output. A low TCI indicates strong environmental performance with minimal emissions per unit of energy supplied, demonstrating alignment with decarbonization targets. Conversely, a higher value signals greater carbon intensity, suggesting opportunities for emission reduction through fuel switching or increased electrification with renewable electricity. This metric serves as a key indicator for tracking progress toward climate goals and informing technology selection and policy decisions.

Tables 2 and 3 summarize the KPI framework developed in this analysis, integrating established, adapted, and novel metrics. The flexibility indicators are structured along three complementary dimensions,

Table 2
Flexibility indicators.

Indicator	Purpose	Range	Ref.
Electricity Consumption Response (ECR)	relative change in electricity consumption under variable vs. constant prices; indicates ability for price-responsive dispatch flexibility	– (%)[a]	cf. [55]
Peak Load Adjustment (PLA)	relative change in peak electricity demand under variable pricing; assesses peak shaving potential to reduce grid strain	– (%)[a]	cf. [56]
Operational Flexibility Range (OFR)	quantifies operational adaptability via convex hull area of normalized electricity vs. thermal supply; larger range indicates greater flexibility	0 to 1 (–)[b]	cf. [57]
Thermal Generation Utilization Rate (TGUR)	evaluates utilization of thermal generation capacity (0% = unused, 100% = full load); low values = limited downward flexibility; high values = limited upward flexibility	0 to 100 (%)[b]	cf. [58]
Storage to Peak Ratio (SPR)	relates storage energy capacity to peak demand (hours of possible peak supply if fully charged); indicates capability for temporal load shifting	0 to 3000 (h)[c]	cf. [59]
Thermal Storage Utilization Factor (TSUF)	assesses storage cycling intensity (0% = unused, 100% = max throughput); high values = active load balancing; low values = underutilized	0 to 100 (%)[b]	–

[a] Novel indicator; no direct literature precedent.
[b] Range based on technical system constraints.
[c] Range based on literature benchmarks.

Table 3
System performance and sustainability indicators.

Indicator	Purpose	Range	Ref.
Levelized Cost of Thermal Energy (LCOT)	calculates break-even price per MWh for long-term economic viability; enables cost benchmarking across systems	10 to 288 (€/MWh_{th})[b]	[60]
Electrification Share (ES)	measures share of thermal energy from electricity-dependent technologies; high share = higher flexibility potential for sector coupling	0 to 100 (%)[a]	–
Thermal Carbon Intensity (TCI)	quantifies CO_2 emissions per thermal energy; assesses environmental performance and decarbonization progress	30 to 120 (kg CO_2/MWh)[b]	[20]

[a] Range based on technical system constraints.
[b] Range based on literature benchmarks.

with two indicators addressing each dimension. Price response is assessed through ECR and PLA, capturing changes in aggregate electricity consumption and peak demand, respectively. Operational adaptability is characterized by OFR and TGUR, quantifying the breadth of feasible operating points and the availability of capacity headroom for load adjustment. Storage dynamics are assessed via SPR and TSUF, distinguishing installed storage shifting potential from its actual utilization in operation. Using paired indicators for each dimension helps reduce the risk of misleading interpretations based on a single metric. For example, a system may exhibit limited net consumption change under variable prices while still providing substantial temporal flexibility through active storage cycling.

Established indicators are adopted from the literature to provide validated benchmarks, while adapted indicators draw on existing concepts and extend them to the DHC flexibility context. Novel indicators are introduced to capture previously unmeasured dimensions of system flexibility. The origin of each indicator is specified at its introduction in Sections 3.1.2 and 3.1.3. Where available, the tables include literature-based comparative ranges, with a detailed discussion provided in Section 5.

The ranges reported in Tables 2 and 3 define benchmark categories (favorable, acceptable, unfavorable) that serve as interpretive guidelines for comparative analysis within a given system. As no established benchmark ranges exist for DHC flexibility assessment, these thresholds are approximate and illustrative, intended to support structured comparisons rather than absolute evaluations. Threshold values are derived from three sources: (i) literature benchmarks for established indicators (LCOT, TCI), where ranges reflect values reported in comparable DHC studies; (ii) technical bounds implied by the indicator definition (ES, TSUF, and TGUR are percentage-based and thus constrained to 0–100 %), combined with materiality-oriented thresholds that distinguish between negligible effects and moderate or intensive activation of flexibility; and (iii) engineering judgement for indicators without established empirical benchmarks (ECR, PLA, OFR, SPR), informed by the expected magnitude of effects and temporal flexibility horizons. For the latter category, thresholds are set to distinguish orders of magnitude rather than to define precise cutoffs. Their primary function is to separate negligible effects from moderate responses, and moderate responses from substantial, system-level impacts.

For most indicators, the direction of improvement is intuitive: lower costs (LCOT), lower emissions (TCI), higher electrification (ES), and more active storage cycling (TSUF) are favorable. Some indicators require explicit clarification to avoid misleading interpretation. ECR thresholds are symmetrical around zero because price-responsive behavior is indicated by both positive and negative responses. Flexibility is determined by the magnitude of the change, not its direction. The boundaries separate consumption changes attributable to normal operational variability from those indicating active price-responsive dispatch, with the outer threshold marking responses that would be considered substantial in the context of demand-side flexibility activation. PLA boundaries are asymmetric because peak reduction supports grid stability, while peak increases impose system costs. The reduction threshold reflects a level of peak shaving that would meaningfully contribute to grid relief, while the increase threshold marks a point beyond which system operators would likely consider the demand pattern problematic. TGUR is evaluated as favorable in the mid-range, as moderate utilization preserves capacity reserves for both upward and downward flexibility; extreme values indicate asymmetric flexibility potential. SPR thresholds reflect temporal flexibility horizons, distinguishing limited short-term buffering from substantial multi-hour to multi-day load shifting capability. For OFR, thresholds are informed by the observed case study results and remain preliminary given the absence of external

benchmarks for this convex-hull-based metric; the boundaries are scaled to distinguish negligible operational variation from meaningful dispersion across scenarios. These categories primarily serve as visual aids for cross-scenario comparison and should be adjusted to local conditions when applying the framework elsewhere. In practice, when applying the framework to a specific system context, users may need to adjust threshold values based on local climate conditions, available technology portfolios, grid characteristics and prevailing market structures. For instance, systems in regions with high price volatility or extensive storage capacity may require broader ranges for price-response indicators, while those in cooling-dominated climates may necessitate adjusted benchmarks for cooling-related metrics. The framework's strength lies in its adaptability: it provides a consistent methodological structure for comparing DHC configurations within a given context, without imposing fixed performance targets. Future applications of the framework to diverse case studies will help validate and refine these thresholds, ultimately enabling more context-sensitive benchmark ranges.

3.2. Concrete implementation/Showcase

The structure of this section is twofold. First, the modeling framework, comprising two distinct models, is described succinctly in Sections 3.2.1 and 3.2.2. The first model generates electricity price profiles at the country level, while the second model uses these hourly price profiles as input to calculate the cost-optimal energy supply at the district-level. The two models are soft-linked unidirectionally, with electricity price profiles being the only data exchanged between them. This approach treats the DHC system as a price taker, since district-level consumption represents a negligible share of national electricity demand, making feedback effects on wholesale prices insignificant. The models are selected for their suitability as data generators within the proposed framework. GENeSYS-MOD provides scenario-consistent price profiles, and DESPO captures investment robustness and operational flexibility across multiple scenarios. These are interchangeable components, and alternative models or empirical data sources can be used instead, provided the necessary KPI input variables are available. Next, the empirical case study is outlined in Section 3.2.3.

3.2.1. Global energy system model (GENeSYS-MOD)

This subsection briefly describes GENeSYS-MOD, which was used to generate hourly electricity prices at the country level. It is an open-source, multi-energy carrier, energy system model and is specialized in investigating long-term pathways for the energy system. It does so by minimizing the total costs of the energy system over a selected modeling period for a specified set of regions. A key strength of this model is its comprehensive, cross-sectoral approach, covering electricity, buildings, industry, and transport while accounting for sector coupling and inter-regional energy trade. Energy demands are predefined, and the model makes cost-optimal investment decisions regarding capacity expansion across different technologies to meet them across all sectors and time steps. Readers interested in the complete mathematical formulation, are referred to relevant publications [61,62] and the detailed documentation of GENeSYS-MOD [63,64].

Temporal Resolution and Dispatch Component: The model outputs are normally issued for representative periods, where input data is aggregated into a smaller number of consecutive timeslices to reduce computational complexity. For this study the power system dispatch model component of GENeSYS-MOD is employed, as it operates on a full hourly basis. This provides a high-resolution analysis of the system's ability to meet electricity demand in each region and for every hour of a given year. It takes the output from GENeSYS-MOD, such as power demand, installed capacities, transmission lines, and energy storage, and optimizes dispatch for minimal costs. While this hourly resolution is a major advantage for capturing price volatility, one limitation must be noted: When the installed capacity is insufficient to meet the demand, the model can use an extremely costly, infeasible technology to provide electricity. This ensures that the model always finds a feasible solution, and highlights potential shortcomings in the GENeSYS-MOD outputs.

For this analysis, hourly electricity prices were derived from the dual variables of the dispatch model. These prices are used as input for the DHC model, which is described more thoroughly in the subsequent section. This data was obtained for four different storylines derived from the European Energy Vision 2060 study [65]. While each scenario describes a different pathway for decarbonizing the European energy system, results are presented for one storyline only.

3.2.2. The district energy stochastic portfolio optimization model (DESPO)

The model described in this section is formulated as a two-stage stochastic mixed-integer linear program, designed to determine the cost-optimal heating and cooling supply technology portfolio at the district level. A key strength of this approach is its ability to capture both long-term investment robustness and short-term operational flexibility - critical for assessing how DHC systems can contribute to power system flexibility. The objective function minimizes the total costs of DHC supply, integrating investment, fixed and variable costs per technology. While the full mathematical formulation—including all constraints and variables—is available [66], this section focuses on a narrative description of the model's key components. Only case study-specific contributions are explicitly introduced in the main text. For readers interested in more detailed formulation, Zwickl-Bernhard et al. [57] offers a comprehensive reference.

Heating and Cooling Technology Portfolio: For the purpose of this study, 13 different technologies are modeled, including 7 heat generation technologies, 3 cooling generation technologies, and 3 TES systems. This diverse technology portfolio is another major advantage, as it allows for a comprehensive evaluation of renewable heat integration options. The modeling approach incorporates the possibility of investing in tank TES and ice TES systems. Moreover, a special feature of the analyzed case study, which will be described in the following section, is its ability to incorporate seasonal TES in the form of a borehole TES. Since the focus is on renewable heat sources, particular attention is given to environmental factors that significantly impact these technologies, such as solar radiation for solar thermal systems, and temperature profiles for large-scale HPs. An overview of the complete technology set included in the model is provided in Appendix A.1 (Table 12). The corresponding evolution of optimal installed capacities across planning periods is reported in Appendix B.1 (Figs. 3 and 4).

One limitation of this approach is that the stochastic optimization's complexity may pose challenges for stakeholders lacking access to specialized tools or expertise. Additionally, while Norwegian district heating typically employs seawater heat pumps, this study models air-source heat pump performance characteristics with temperature-dependent COP profiles as a proxy for large-scale heat pump operation. This simplification provides conservative efficiency estimates given seawater's more stable thermal properties.

Scenarios and Data: The data used in this study consist of information for calculating the heating and cooling demand in the analyzed district and for determining the cost-optimal DHC supply. The heating and cooling demand profiles used as the main input for the portfolio optimization were generated using PROFet [67]. As mentioned above electricity prices were derived from GENeSYS-MOD, while historical monthly and quarterly natural gas prices have been used and future prices for annual CO_2 emissions have been extracted from the European Parliament emission goals [68]. For this study a time horizon of 15 years (from 2025 until 2040) is used, divided into five-year planning periods, which include two expansions of the DHC system in 2030 and 2035.

This study examines 15 distinct scenarios, reflecting variations in energy demand, prices (e.g., electricity, natural gas), regulatory measures (e.g., carbon pricing, renewable incentives), and other parameters. The scenario design builds on the approach by Zwickl-Bernhard et al. [57], who define comparable scenarios for a district energy system in Washington, D.C., and has been slightly adapted for this study. The

Table 4
Overview of the scenario definitions and key parameter variations (analysis horizon until 2040).

Scenario	Narrative and key parameter variation	Probability (%)
(1) *Reference*	Baseline assumptions regarding energy and regulatory policies, as well as economic and other input parameters, until 2040. This scenario represents the most likely development pathway.	15
(2) *High Electricity Prices*	Wholesale and retail electricity prices are 20% higher than baseline assumptions until 2040 ($1.2 \times c^{\text{elec}}_{1,y,h}$).	5
(3) *Low Electricity Prices*	Wholesale and retail electricity prices are 20% lower than in the reference scenario until 2040 ($0.8 \times c^{\text{elec}}_{1,y,h}$).	5
(4) *Flexible Electricity Market*	Hourly electricity prices are strictly non-negative due to high flexibility provision by other market participants, such as batteries ($c^{\text{elec}}_{4,y,h} \geq 0$).	10
(5) *Energy Price Peaks*	Substantial price increases for natural gas (20%) and electricity (10%) occur during 2035–2039 due to high demand and limited supply ($1.2 \times c^{\text{gas}}_{1,y,h}$; $1.1 \times c^{\text{elec}}_{1,y,h}$).	6
(6) *Green-Friendly*	Focus on renewable energy sources and carbon pricing. A 20% reduction in specific investment costs incentivizes clean technologies, while a 10% increase in carbon prices raises costs for carbon-emitting technologies ($0.8 \times \bar{c}^{\text{inv}}_{1,y}$; $1.1 \times c^{\text{CO}_2}_{1,y}$) until 2040.	6
(7) *Low Gas Demand*	A 25% increase in carbon prices reduces natural gas demand, lowering gas prices by 5% and electricity prices by 15% until 2040 ($0.95 \times c^{\text{gas}}_{1,y,h}$; $0.85 \times c^{\text{elec}}_{1,y,h}$).	6
(8) *Natural Gas Friendly*	Reduced natural gas prices combined with the absence of carbon pricing in 2040 ($0.85 \times c^{\text{gas}}_{1,y,h}$; $c^{\text{CO}_2}_{8,y} = 0$).	3
(9) *Cold Winters*	Heating demand increases by 10% due to colder-than-average winters in 2040 ($1.1 \times Q^{\text{heat}}_{1,y,h}$).	10
(10) *Hot Summers*	Increased cooling demand (10%) due to higher-than-average summer temperatures during the 2030s ($1.1 \times Q^{\text{cool}}_{1,y,h}$).	10
(11) *Warm Summers*	A minor increase in cooling demand (5%) in 2040 ($1.05 \times Q^{\text{cool}}_{1,y,h}$).	3
(12) *Moderate Climate*	Milder summers and warmer winters reduce heating and cooling demand by 10% each until 2040 ($0.9 \times Q^{\text{cool}}_{1,y,h}$; $0.9 \times Q^{\text{heat}}_{1,y,h}$).	3
(13) *Delayed Carbon Price*	No carbon pricing until 2035, followed by moderate carbon price increases until 2040.	2
(14) *High Carbon Price*	Carbon prices increase by 25% relative to the reference scenario until 2040 ($1.25 \times c^{\text{CO}_2}_{1,y}$).	10
(15) *Expiring RES Support*	Financial support for renewable energy investment costs expires after 2034 ($0.7 \times \bar{c}^{\text{inv}}_{1,y}$).	6

scenarios and their parameters can be further adjusted when applying the framework to other contexts. Scenario-specific probabilities are expert-informed estimates derived from a structured review of district energy scenarios in the literature [57]. These scenarios are exploratory in nature, and no formal statistical inference is attempted. Refining probability estimation methods remains an area for future improvement. Detailed definitions of all scenarios are provided in Table 4 below. The model generates separate results for each of the 15 scenarios, primarily affecting the dispatch of the technologies, depending on their installed capacities.

3.2.3. Empirical case

The proposed case study of a small district in Trondheim, Norway, offers a particularly relevant examination of how DHC systems can provide sustainable heating and cooling solutions. A key strength of this case study is its empirical grounding and transferability: Nyhavna, a former industrial harbor currently undergoing redevelopment, has already been examined in previous research [69], enabling direct comparability and validation of our results. Its development will be carried out in three construction phases, with detailed information on floor areas and infrastructure expansion available in the aforementioned study.

Nyhavna currently lacks heating or cooling infrastructure and significant geothermal resources. Nevertheless, this area presents unique advantages for flexibility analysis in this context: Trondheim's existing DH network passes close by, and Nyhavna has the potential for seasonal TES through a borehole TES system. This system could be charged primarily by surplus heat from a nearby waste incineration plant, allowing for large-scale summer-to-winter heat storage; a critical feature for assessing long-term flexibility potential. In addition, a large seawater-based HP will be installed, further increasing the portfolio of flexibility assets.

Nyhavna is a particularly well-suited location for this analysis due to two key factors. First, Norway's heating sector is highly electrified [16]. This makes it an ideal environment in which to study how DHC systems can interact with and support the electricity grid. Second, Nyhavna's planned development in three phases and its potential for seasonal TES integration provide a realistic framework to evaluate flexibility provision over time. The existing literature on Nyhavna further strengthens the practical relevance and transferability of this study's findings and supports the validation of its KPI framework.

Several framework considerations warrant attention. Some flexibility KPIs represent novel metrics and their categorization thresholds rely on educated estimates, introducing interpretive subjectivity. The framework employs hourly temporal resolution, consistent with standard energy system modeling, which captures consumption flexibility and load shifting but precludes sub-hourly ancillary services. While the framework itself is technology- and context-agnostic, its application requires adaptation of the technology portfolio to local conditions, including available resources (e.g., geothermal potential, waste heat), climate patterns, and grid characteristics. Consequently, indicator magnitudes are inherently case-specific and should not be interpreted as universal performance targets. When applying the framework, results can be interpreted along two complementary dimensions: (i) cross-scenario comparisons within the same system, which highlight the sensitivity and robustness of flexibility provision under varying external conditions, and (ii) temporal comparisons across planning periods, which

Table 5
Flexibility indicators for the base scenario (2030) with benchmark ranges. Black arrows indicate system-wide indicators, while red and blue arrows show heating- and cooling-specific ranges for subsystem-specific indicators.

System-wide indicators	Unit	Value	Range
Electricity Consumption Response (ECR)	%	-14.35	±20 ±5 favorable acceptable unfavorable
Peak Load Adjustment (PLA)	%	0	−10 +5 favorable acceptable unfavorable

Subsystem-specific indicators	Unit	Heat	Cool	Range
Operational Flexibility Range (OFR)	–	1.42×10^{-2}	1.51×10^{-5}	0.05 .01 favorable acceptable unfavorable
Thermal Generation Utilization Rate (TGUR)	%	49.52	8.60	20 40 60 80 unfav. acc. fav. acc. unfav.
Storage to Peak Ratio (SPR)	h	2.87	17.06	200 0 favorable acceptable unfavorable
Thermal Storage Utilization Factor (TSUF)	%	39.50	9.28	60 20 favorable acceptable unfavorable

demonstrate how flexibility evolves alongside system expansion and technology deployment. The framework's primary value lies in enabling these systematic, context-driven comparisons rather than establishing rigid, absolute benchmarks. To further strengthen the empirical foundation of the proposed benchmark categories, future research should explore cross-case applications across diverse geographic and regulatory contexts.

4. Results

This section presents the evaluation of the proposed KPI framework applied to the DHC system in Nyhavna. Section 4.1 examines the base scenario (Scenario 1 *Reference*), representing the most probable development pathway, with a detailed assessment of 2030 results followed by the temporal evolution of selected indicators until 2040. Section 4.2 extends this foundation by comparing KPI outcomes across six representative scenarios for 2030, revealing how flexibility provision and system performance respond to varying energy policies, technological conditions, and demand patterns.

4.1. Base scenario

4.1.1. 2030

The flexibility indicators in Table 5 reveal that operational flexibility in 2030 is dominated by the heating subsystem, which exhibits moderate operational flexibility, while cooling contributes negligibly. This pronounced asymmetry reflects Norway's climate-driven energy profile, where heating demand vastly exceeds cooling requirements, a pattern that persists across subsequent flexibility metrics. Although the system achieves a 14% reduction in electricity consumption through price-responsive operation, its failure to reduce peak load is a critical limitation for grid support.

The system's electricity use responds moderately to price signals, achieving an ECR of −14.35%. This reduction occurs through strategic dispatch adjustments that shift load from high-price to low-price periods, supporting grid balancing through price arbitrage without compromising thermal supply.

This consumption flexibility, however, does not extend to peak demand periods, as demonstrated by a PLA of 0% falling into the unfavorable range. Peak electricity consumption remains unchanged regardless of price signals, indicating that maximum demand events are driven by extreme thermal load requirements rather than economic incentives. The inability to modulate peak loads is a fundamental limitation that prevents the system from providing grid peak shaving services. This is likely due to a temporal mismatch between thermal demand and price peaks.

The OFR reveals a significant difference between subsystems, with heating achieving 1.42×10^{-2} (acceptable range) while cooling registers only 1.51×10^{-5} (unfavorable range). Fig. 2 illustrates this contrast by showing the OFR of the heating and cooling subsystems, based on normalized electricity consumption and thermal supply, for all scenario–year combinations.

As Fig. 2(a) shows, the heating subsystem has a broad convex hull, which indicates a wide operational envelope and a high degree of flexibility. This reflects the ability of heating technologies to operate across diverse electricity consumption levels under varying system conditions. In contrast, Fig. 2(b) demonstrates that the cooling subsystem operates within a highly constrained band, with data points tightly clustered along a narrow trajectory. This limited dispersion highlights the comparatively minor contribution of cooling to overall system flexibility.

The TGUR reveals distinct operational characteristics for the heating and cooling subsystems. Heating operates at 49.52%, which falls within the favorable range, indicating a balanced utilization that preserves significant flexibility potential for both increased and decreased dispatch as needed. In contrast, cooling's TGUR of 8.60% is classified as unfavorable, reflecting its sporadic operation limited to peak summer days.

The SPR reveals contrasting buffering capacities, with heating at 2.87 hours and cooling at 17.06 hours. Heating storage demonstrates limited potential for covering peak demand periods, constraining the system's ability to decouple thermal supply from electricity consumption during critical grid situations. This low ratio reflects insufficient price arbitrage opportunities when thermal peaks and electricity price peaks are temporally misaligned, limiting economic incentives for storage investment. Cooling storage exhibits higher flexibility potential, though practical utilization remains limited in this climate context.

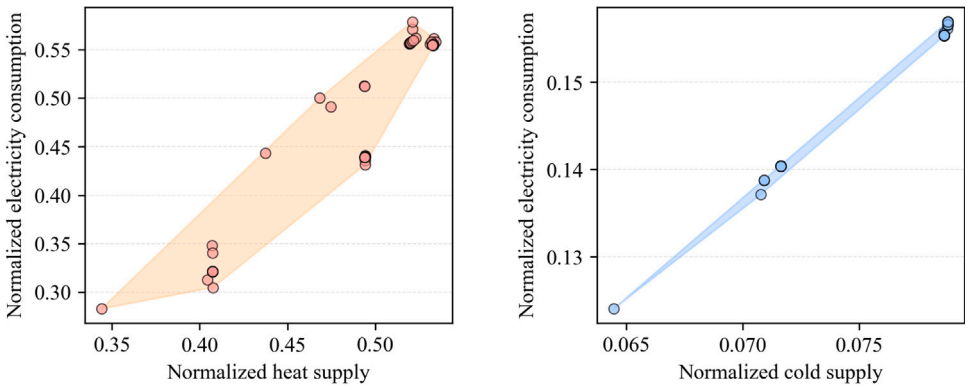

(a) Heat flexibility (b) Cool flexibility

Fig. 2. Operational flexibility range (OFR) for heating and cooling subsystems, showing normalized electricity consumption versus thermal supply across all scenario–year combinations.

Table 6
System performance and sustainability indicators for the base scenario (2030). Red and blue arrows show heating- and cooling-specific ranges for subsystem-specific indicators.

Indicator	Unit	Heat	Cool	Range
Levelized Cost of Thermal Energy (LCOT)	€/MWh$_{th}$	34.49	84.59	40 80 favorable acceptable unfavorable
Electrification Share (ES)	%	88.49	100	60 20 favorable acceptable unfavorable
Thermal Carbon Intensity (TCI)	kg CO$_2$/MWh$_{th}$	74.45	6.35	40 100 favorable acceptable unfavorable

The TSUF of 39.50% for heating and 9.28% for cooling confirms disparate storage engagement. Heating storage cycles regularly for load balancing and price arbitrage, while cooling storage remains largely dormant throughout the year. This pattern confirms heating storage actively enables temporal flexibility, whereas cooling infrastructure serves occasional peak requirements.

The system performance and sustainability indicators in Table 6 reveal contrasting performance profiles between subsystems, with heating achieving economically competitive operation while cooling exhibits elevated unit costs despite favorable environmental performance. Both subsystems demonstrate strong electrification enabling sector coupling, yet create direct exposure to electricity market volatility and grid carbon intensity.

Economic performance diverges substantially between subsystems. Heating achieves 34.49 €/MWh$_{th}$ (acceptable range), while cooling reaches 84.59 €/MWh$_{th}$ (unfavorable range). Heating demonstrates economically viable operation benefiting from high annual utilization that distributes fixed costs across substantial energy output. The elevated unit costs for cooling stem from minimal annual demand concentrated in summer months, forcing fixed infrastructure investments to be recovered through limited energy delivery.

Both subsystems demonstrate strong electrification, with heating at 88.49 % and cooling at 100.00 %, establishing substantial coupling between thermal and electricity sectors. This high electrification enables flexibility provision through consumption modulation responsive to grid conditions and renewable generation patterns. The configuration creates direct exposure to electricity price volatility, with operational costs and carbon emissions closely tied to grid conditions.

Carbon emissions reflect technology composition and Norway's low-carbon grid, with heating at 74.45 kg CO$_2$/MWh$_{th}$ (acceptable range) and cooling at 6.35 kg CO$_2$/MWh$_{th}$ (favorable range). Heating's carbon footprint combines emissions from waste incineration with grid electricity consumed by electric technologies. Cooling achieves near-zero emissions through complete electrification paired with Norway's hydropower-dominated grid, demonstrating that full electrification with clean electricity enables minimal thermal supply emissions.

4.1.2. *Temporal evolution by 2040*

The temporal evolution of KPIs reflects both system expansion, with capacity investments in 2030 and 2035 in response to increased thermal demand resulting from phased district development (see Appendix B.1), and operational maturation over the planning horizon as reflected in the temporal KPI trends (Appendix B.2). An analysis of the flexibility indicators in Table 7 demonstrates that heating flexibility undergoes substantial transformation through storage capacity expansion and increased generation utilization, while cooling exhibits negligible evolution. The system's inability to modulate peak electricity loads persists throughout the entire planning horizon, confirming a fundamental structural limitation.

The ECR demonstrates non-monotonic evolution, beginning at 5.94% (unfavorable) in 2025, transitioning to −14.35% (acceptable) in 2030, then returning to positive values by 2040 (2.91%, unfavorable). This trajectory reveals fundamental shifts in operational strategy. The negative response in 2030 demonstrates consumption reduction through strategic technology switching, while the return to positive values reflects maturation toward storage-dominated flexibility provision, where expanded capacity enables intensified electricity consumption during low-price periods for subsequent discharge.

The capability for PLA remains fundamentally absent throughout the planning horizon, with values at 0% in 2025–2030, rising marginally to

Table 7
Temporal evolution of flexibility indicators for the base scenario (2025–2040). Horizontal bars show the range from minimum to maximum values across all years, with tick marks indicating the start year (2025) and triangles the end year (2040). Black bars represent system-wide indicators; red and blue bars denote heating and cooling subsystems, respectively.

Indicator	Sec.	Unit	2025	2030	2035	2040	Range
Electricity Consumption Response (ECR)	–	%	5.94	−14.35	1.33	2.91	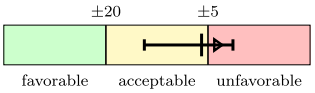
Peak Load Adjustment (PLA)	–	%	0.00	0.00	0.15	0.27	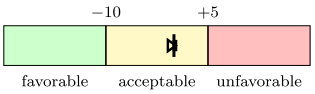
Thermal Gen. Utilization Rate (TGUR)	Heat	%	41.18	49.52	54.20	54.35	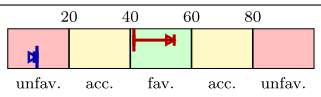
	Cool		9.54	8.60	9.50	9.47	
Storage to Peak Ratio (SPR)	Heat	h	3.39	2.87	5.54	9.58	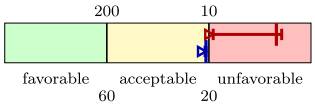
	Cool		15.47	17.06	15.51	15.51	
Thermal Storage Utilization Factor (TSUF)	Heat	%	21.14	39.50	36.09	24.30	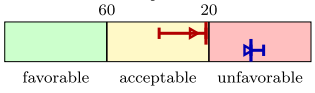
	Cool		11.76	9.28	11.58	11.47	

0.27% by 2040 (all unfavorable range). This persistent near-zero performance confirms that peak electricity demand is structurally constrained by thermal load requirements, preventing effective modulation regardless of technology portfolio evolution or storage capacity expansion.

The TGUR for heating increases from 41.18% (2025) to 54.35% (2040), reflecting proportional capacity expansion with demand growth while maintaining consistent reserve margins for operational flexibility. Cooling utilization remains stable at 8.60–9.54%.

The SPR for heating follows a distinct temporal pattern, decreasing from 3.39 hours (2025) to 2.87 hours (2030) before expanding significantly to 9.58 hours by 2040. While these values remain in the unfavorable range, the 2040 expansion approaches the acceptable threshold, indicating progressive investments in temporal flexibility. However, storage capacity remains insufficient for comprehensive peak coverage. Cooling storage ratios, in contrast, stabilize within the acceptable range (15–17 hours), reflecting consistent operational characteristics without significant trends over time.

The TSUF patterns reveal a persistent challenge where capacity deployment outpaces operational optimization. Heating utilization nearly doubles from 21.14% in 2025 to 39.50% in 2030, then declines to 24.30% by 2040 despite continued capacity growth. This non-monotonic pattern indicates that newly installed infrastructure remains partially idle, as operational strategies lag behind infrastructure deployment. Cooling storage utilization remains stable near 10%, consistent with minimal operational engagement.

As shown in Table 8, the system performance and sustainability indicators demonstrate that heating experiences significant decarbonization through rapid electrification between 2025 and 2030, enabling dramatic carbon intensity reductions that subsequently moderate in later years. Meanwhile, cooling maintains stable, low-carbon performance throughout the planning horizon.

Heating electrification undergoes substantial transformation during the initial development period, with ES increasing from 65.11% (favorable) in 2025 to 88.49% in 2030, then continuing above 95% by 2035–2040 (favorable). This rapid early expansion reflects the strategic prioritization of electric technologies to enhance flexibility provision and support decarbonization objectives. Cooling remains fully electrified throughout the period.

The TCI reduction is most dramatic during the initial phase, with heating TCI dropping from 190.82 kg CO_2/MWh (unfavorable) in 2025 to 74.45 kg CO_2/MWh (acceptable) in 2030, representing a 61% decrease. Further reductions to 39.67 kg CO_2/MWh (favorable) occur by 2035, though values rise slightly to 42.53 kg CO_2/MWh (acceptable) by 2040. This trajectory reflects rapid electrification displacing conventional technologies, followed by stabilization as the system approaches practical decarbonization limits. This is driven by the evolution of the installed technology mix (Appendix B.1) and the applied technology-specific emission factors (Appendix A.2). Cooling emissions remain stable near 6.4 kg CO_2/MWh (favorable) throughout, reflecting consistent full electrification.

4.2. Cross-scenario comparison for 2030

The stochastic optimization framework enables analysis of system performance across diverse market, climate, and policy environments, revealing the operational range and sensitivity of flexibility provision. Of the 15 scenarios examined, six representative cases are selected for detailed comparison in 2030: *Reference* (1), *High Electricity Prices* (2), *Green-Friendly* (6), *Cold Winters* (9), *Hot Summers* (10), and *High Carbon Price* (14). These scenarios were selected to represent distinct scenario clusters, covering market-based price variations (2), policy-driven conditions (6, 14), and climate-induced demand shifts (9, 10). Together, they represent 56% of the probability-weighted scenario space.

The flexibility indicators in Table 9 reveal remarkable stability across all scenarios. Most indicators exhibit minimal variation despite substantial differences in market prices, climate conditions, and policy frameworks. The heating subsystem maintains consistent operational characteristics, while cooling shows negligible engagement across all conditions.

The ECR demonstrates modest variation, ranging from −14.35 % in the *reference* case to −16.23 % under *Hot Summers* (10). All scenarios maintain negative values, confirming that the system consistently reduces electricity consumption when exposed to variable price signals. The slightly more pronounced response in (10) reflects elevated cooling demand enabling more aggressive load shifting, while *High Electricity Prices* (2) intensify economic incentives for consumption reduction.

Table 8
Temporal evolution of system performance indicators for the base scenario (2025–2040). Horizontal bars show the range from minimum to maximum values across all years, with tick marks indicating the start year (2025) and triangles indicating the end year (2040). Red and blue bars denote heating and cooling subsystems, respectively.

Indicator	Sec.	Unit	2025	2030	2035	2040	Range
Electrification Share (ES)	Heat	%	65.11	88.49	95.78	95.31	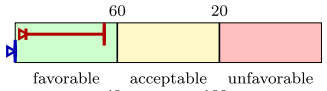
	Cool		100.00	100.00	100.00	100.00	
Thermal Carbon Intensity (TCI)	Heat	$kg\,CO_2$ / MWh_{th}	190.82	74.45	39.67	42.53	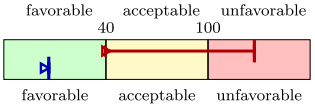
	Cool		6.41	6.35	6.44	6.46	

Table 9
Flexibility indicators across selected scenarios (2030). Black whiskers indicate system-wide indicators, while red and blue show heating- and cooling-specific ranges for subsystem-specific indicators.

Indicator	Sec.	Unit	(1) *Reference*	(2) *High Price*	(6) *Green Friendly*	(9) *Cold Winters*	(10) *Hot Summers*	(14) *High Carbon*	Range
Electricity Consumption Response (ECR)	–	%	−14.35	−15.38	−14.69	−14.76	−16.23	−14.80	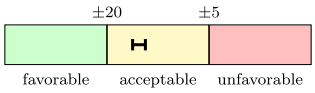
Peak Load Adjustment (PLA)	–	%	0.00	0.00	0.00	0.00	0.00	0.00	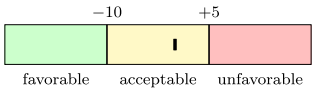
Thermal Gen. Utilization Rate (TGUR)	Heat	%	49.52	49.48	49.52	49.50	49.49	49.49	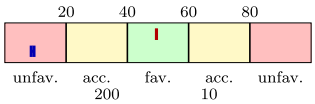
	Cool		8.60	8.60	8.60	8.60	9.52	8.60	
Storage to Peak Ratio (SPR)	Heat	h	2.87	2.87	2.87	2.87	2.87	2.87	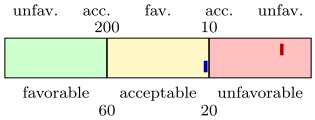
	Cool		17.06	17.06	17.06	17.06	15.51	17.06	
Thermal Storage Utilization Factor (TSUF)	Heat	%	39.50	44.33	39.50	39.50	43.30	39.50	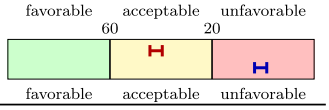
	Cool		9.28	9.28	9.28	9.28	11.67	9.28	

The narrow range indicates fundamentally stable response mechanisms regardless of external conditions.

Peak load modulation capability remains universally absent, with PLA at 0% (unfavorable range) across all scenarios. This persistent inflexibility confirms that peak demand events are primarily driven by fixed thermal load requirements rather than economic or policy incentives. The system's inability to provide grid peak shaving services remains unchanged regardless of price levels, climate extremes, or regulatory frameworks.

The TGUR displays impressive consistency across various scenarios, with heating maintaining a steady 49.49%–49.52%, well within the favorable range. Cooling utilization remains consistently low at around 8.6%, except in the *Hot Summers* scenario (10), where it rises modestly to 9.52% due to increased demand. This minimal variation confirms a balanced capacity configuration that ensures reliable operation while maintaining substantial reserve margins for flexible grid services under diverse external conditions.

The SPR remains invariant at 2.87 hours for heating and 17.06 hours for cooling across all scenarios except *Hot Summers* (10), where cooling decreases slightly to 15.51 hours. This stability reflects identical installed storage capacity and similar peak demand profiles across most scenarios. The reduction of the cooling SPR in (10) reflects the cooling demand increase in this scenario, while storage capacity remains unchanged, demonstrating how demand shifts alter the SPR even with fixed infrastructure.

The TSUF exhibits selective sensitivity, responding primarily to price signals and climate extremes. Heating storage increases from baseline 39.50% to 44.33% under *High Electricity Prices* (2) and 43.30% during *Hot Summers* (10), reflecting intensified temporal arbitrage when economic incentives strengthen. Cooling storage similarly rises from 9.28% to 11.67% in (10). Green investment support (6), *Cold Winters* (9), and emission pricing (14) leave utilization unchanged, indicating these policy frameworks do not alter optimal dispatch strategies.

The system performance and sustainability indicators in Table 10 reveal contrasting sensitivity to scenarios. Economic performance varies substantially, with LCOT differing by 15%–24% between investment support and emission pricing mechanisms, while ES and TCI remain remarkably stable, demonstrating that flexibility and environmental characteristics are structurally determined rather than policy-responsive.

LCOT exhibits the strongest variation among all indicators, revealing significant economic sensitivity to policy frameworks. Heating costs range from 32.31 €/MWh_{th} (acceptable) under green investment support (6) to 37.29 €/MWh_{th} (acceptable) with ambitious CO_2 pricing (14), representing a 15% variation. Cooling demonstrates even more pronounced sensitivity, ranging from 68.31 €/MWh_{th} (acceptable) in (6) to approximately 84–85 €/MWh_{th} (unfavorable) in other scenarios, reflecting nearly a 24% variation. This amplified cooling response stems from low utilization that magnifies the importance, making investment support particularly effective while other scenarios cluster tightly regardless of price levels or climate conditions.

ES shows exceptional stability, with heating varying by less than 0.1 percentage point (88.43–88.49%) and cooling remaining consistently at 100% across all scenarios. This minimal variation

Table 10
System performance and sustainability indicators across selected scenarios (2030). Red and blue whiskers indicate heating- and cooling-specific ranges for subsystem-specific indicators.

Indicator	Sec.	Unit	(1) *Reference*	(2) *High Price*	(6) *Green Friendly*	(9) *Cold Winters*	(10) *Hot Summers*	(14) *High Carbon*	Range
Levelized Cost of Thermal Energy (LCOT)	Heat	€/MWh$_{th}$	34.49	35.03	32.31	33.93	34.61	37.29	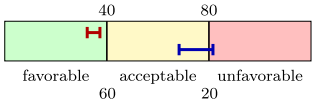
	Cool		84.59	84.74	68.31	84.59	82.70	84.59	
Electrification Share (ES)	Heat	%	88.49	88.47	88.48	88.45	88.46	88.43	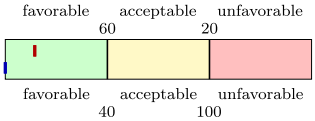
	Cool		100.00	100.00	100.00	100.00	100.00	100.00	
Thermal Carbon Intensity (TCI)	Heat	kg CO$_2$ / MWh$_{th}$	74.45	74.40	74.44	74.62	74.34	74.73	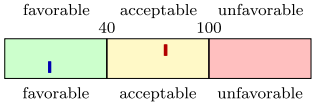
	Cool		6.35	6.35	6.35	6.35	6.43	6.35	

Table 11
Selected indicators with comparable values in existing literature.

Indicator	Range in literature	Reference
Storage to Peak Ratio (SPR)	2–3260 h	[69–72]
Levelized Cost of Thermal Energy (LCOT)	10–288 €/MWh$_{th}$	[20,71,73–77]
Thermal Carbon Intensity (TCI)	30–120 kg CO$_2$/MWh$_{th}$	[77–83]

indicates that the system prioritizes electric technologies regardless of fluctuations in electricity prices, CO_2 costs, or policy incentives. The stability reflects Norway's favorable electrification conditions, particularly its low-carbon electricity grid, suggesting that further electrification gains would require disruptive technological advancements or fundamental shifts in the regulatory landscape.

TCI demonstrates remarkable stability, clustering between 74.34 and 74.73 kg CO$_2$/MWh$_{th}$ for heating and remaining near 6.35 kg CO$_2$/MWh$_{th}$ for cooling across all scenarios. This minimal variation indicates that current operational and policy levers are insufficient to drive significant emission reductions beyond those already achieved through high electrification. Deeper decarbonization would require fundamental technology shifts or further grid decarbonization.

5. Discussion

This section provides a quantitative comparison of our results with literature benchmarks for three indicators where reference values were available: Levelized Cost of Thermal Energy (LCOT), Thermal Carbon Intensity (TCI), and Storage to Peak Ratio (SPR). Table 11 summarizes these reference values from comparable studies. Results show that cost and storage indicators align well with reported ranges, while carbon intensity demonstrates significant temporal evolution from a transitional to a low-carbon performance.

The SPR is benchmarked here using derived literature values calculated from reported storage capacities and peak demand data in comparable studies. For heating, the SPR (2.87–9.58 h) lies at the lower end of the range reported in the existing literature, suggesting limited storage capacity relative to peak demand. This is consistent with systems that rely on short- to medium-term storage rather than seasonal solutions, even though BTES is included. However, the cooling SPR (15.47–17.06 h) falls within the intermediate range, reflecting Norway's low cooling demand and daily storage needs, which are well below seasonal benchmarks.

The heating LCOT (32.3–37.3 €/MWh$_{th}$) aligns with the lower end of the range found in the literature, confirming the competitive cost performance of diversified DHC systems. In contrast, the cooling LCOT (68.3–84.7 €/MWh$_{th}$) is substantially higher, sitting in the mid-range of the benchmark spectrum. This disparity is driven by low utilization factors, reflecting the economic realities of providing cooling in low-demand markets such as Norway.

The TCI for heating shows different benchmark alignment across time periods. Values in the early years (191 kg CO$_2$/MWh$_{th}$) exceed literature benchmarks due to transitional reliance on waste incineration. In later years, the heating TCI (39.7–42.5 kg CO$_2$/MWh$_{th}$) converges with low-carbon benchmarks, indicating successful decarbonization. The cooling TCI (6.35 kg CO$_2$/MWh$_{th}$–6.46 kg CO$_2$/MWh$_{th}$) remains consistently below the values reported in prior studies, reflecting Norway's low-carbon grid.

6. Conclusion

DHC systems represent significant yet underutilized flexibility resources for electricity grids. Despite growing recognition of their potential, systematic assessment and comparison of DHC flexibility capabilities have been hindered by the absence of a consistent quantitative framework. This study addresses this gap by developing and demonstrating a comprehensive framework that integrates flexibility-focused and system performance indicators to enable the systematic evaluation of DHC flexibility provision.

The key contribution of this work lies in shifting the evaluation paradigm from traditional thermal output metrics to flexibility potential assessment. By combining demand-side flexibility indicators with storage dynamics and system performance metrics, the framework yields new insights into the quantifiable flexibility characteristics of DHC systems and their robustness under varying external conditions. It enables decision-makers to systematically compare DHC configurations and quantify not only whether a system provides flexibility, but how much, under what constraints, and at what cost.

Application to a Norwegian case study across 15 scenarios reveals that heating subsystems dominate flexibility provision (ECR reaching 14%) while cooling contributes negligibly in cold climates, and demonstrates remarkable robustness of flexibility indicators despite significant economic performance variations across policy scenarios (LCOT 15–24%).

The framework is designed for grid-coupled, electrified DHC systems where demand-side flexibility can be modulated in response to electricity market signals. While indicator magnitudes are context-specific due to local climate, resources, and grid characteristics, the framework enables systematic comparison of configurations within each setting.

Future research could advance the framework along several directions. First, a price-weighted variant of the ECR could be developed by integrating price differentials into the metric, for example hourly

price deviations from the annual average baseline. This extension would enable a more nuanced evaluation of flexibility provision by distinguishing whether consumption shifts occur during high- or low-price periods, thereby adding an economic efficiency dimension to the current energy-volume perspective. Second, incorporating supply-side flexibility and sub-hourly ancillary services would complement the current focus on consumption-side flexibility and broaden the framework's applicability to a wider range of grid services. Third, investigating the economic valuation of DHC flexibility relative to other grid assets would support the development of flexibility-oriented regulatory frameworks. Additionally, applying the framework across diverse geographic and regulatory contexts would enhance understanding of how local conditions influence flexibility provision capabilities, providing an empirical basis for validating and refining the proposed benchmark categories.

CRediT authorship contribution statement

Leopold Riedl: Writing – review & editing, Writing – original draft, Supervision, Funding acquisition. **Sebastian Zwickl-Bernhard:** Writing – review & editing, Writing – original draft, Supervision, Conceptualization. **Lukas Kranzl:** Writing – review & editing, Writing – original draft, Supervision, Funding acquisition. **Hanne Kauko:** Writing – review & editing, Writing – original draft, Supervision, Project administration, Funding acquisition. **Christopher Schifflechner:** Writing – review & editing, Writing – original draft, Supervision, Project administration, Funding acquisition.

Declaration of generative AI and AI-assisted technologies in the writing process

During the preparation of this work the authors used DeepL and Claude in order to refine the writing. After using these tools, the authors reviewed and edited the content as needed and take full responsibility for the content of the published article.

Declaration of competing interest

The authors declare that they have no known competing financial interests or personal relationships that could have appeared to influence the work reported in this paper.

Acknowledgements

Funding from the European Union's Horizon Europe research and innovation program under grant agreement No. 101147576 (FlexGeo) is gratefully acknowledged. Views and opinions expressed are, however, those of the authors only and do not necessarily reflect those of the European Union or the granting authority. Neither the European Union nor the granting authority can be held responsible for them. The project has also been subsidized through the GEOTHERMICA and JPP Smart Energy Systems Joint Call by the Research Council of Norway and the Austrian Research Promotion Agency via the ERA-NET FLXenabler project (RCN grant agreement No. 341596). The authors acknowledge TU Wien Bibliothek for financial support through its Open Access Funding Program.

Appendices

A. Model input data

A.1. Technology set

Table 12
Overview of heating and cooling technologies and storage systems considered in the analysis.

Generation technology	Input	Output	Short description/key parameter
Electric boiler	Electricity	Heat	Highly dependent on electricity price levels
Gas boiler	Natural gas	Heat	Generates heat only; no electricity required
Air-source heat pump	Electricity	Heat	Efficiency (COP) varies with ambient temperature
Solar thermal	–	Heat	Output depends on solar irradiation
Combined heat and power (CHP)	Natural gas	Heat	Cogeneration prioritizing heat supply over electricity
Industrial excess heat	–	Heat	Availability relies on facility operation
Waste incineration	–	Heat	Converts municipal waste to thermal energy (heat only)
Absorber with cooling tower	Heat	Cold	Chiller using waste heat from plants
Absorber with heat pump	Heat	Cold + Heat	Provides cooling while recovering waste heat
Compression chiller with cooling tower	Electricity	Cold	Compression chiller equipped with a cooling tower
Compression chiller with heat pump	Electricity	Cold + Heat	Provides cooling while recovering waste heat
Air-cooled chiller	Electricity	Cold	Performance depends on ambient air temperature
Tank thermal energy storage	Heat	Heat	Short-term heat storage
Borehole thermal energy storage	Heat	Heat	Serves as summer buffer for waste incineration excess heat
Ice thermal energy storage	Cold	Cold	Stores cold energy

A.2. Emission factors

Table 13
CO_2 emission factors used in thermal carbon intensity (TCI) calculations.

Energy carrier	Emission factor [kg CO_2/MWh]	Source
Natural gas (combustion)	220	[84]
Waste incineration	503	[85]
Norwegian electricity grid	20	[86]

B. Supplementary results

B.1. Installed capacities

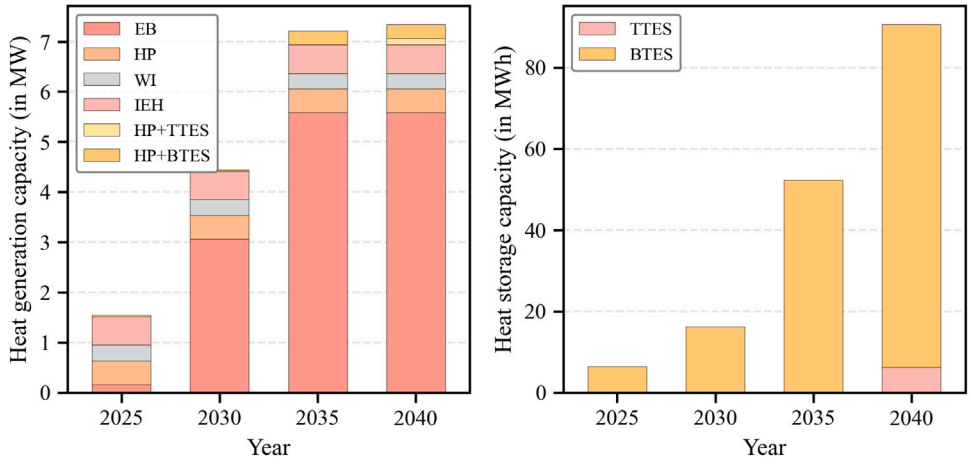

(a) Heat generation (b) Heat storage

Fig. 3. Cumulative installed capacities for heating technologies (2025–2040): (a, left) heat generation and (b, right) heat storage.

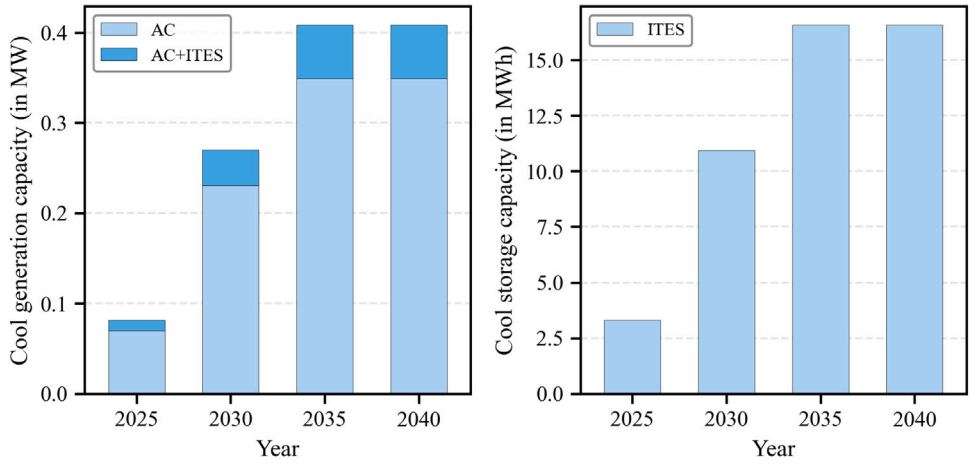

(a) Cool generation (b) Cool storage

Fig. 4. Cumulative installed capacities for cooling technologies (2025–2040): (a, left) Cool generation and (b, right) Cool storage.

B.2. Temporal trends of KPIs

See Figs. 5 and 6.

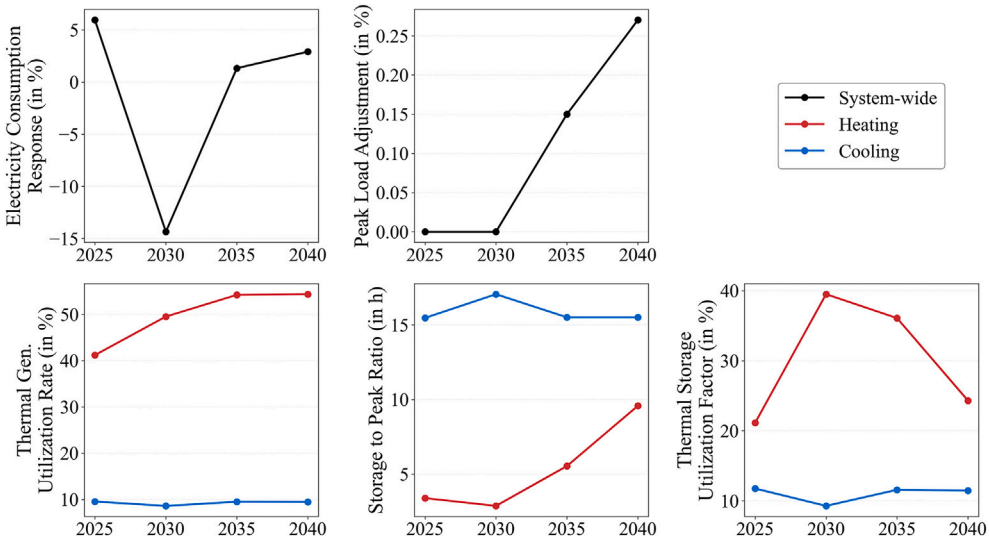

Fig. 5. Temporal evolution of flexibility-related indicators for the base scenario (2025–2040). Subplots depict electricity consumption response (ECR), peak load adjustment (PLA), thermal generation utilization rate (TGUR), storage to peak ratio (SPR), and thermal storage utilization factor (TSUF). Black lines denote system-wide indicators, while red and blue lines represent heating- and cooling-specific values, respectively.

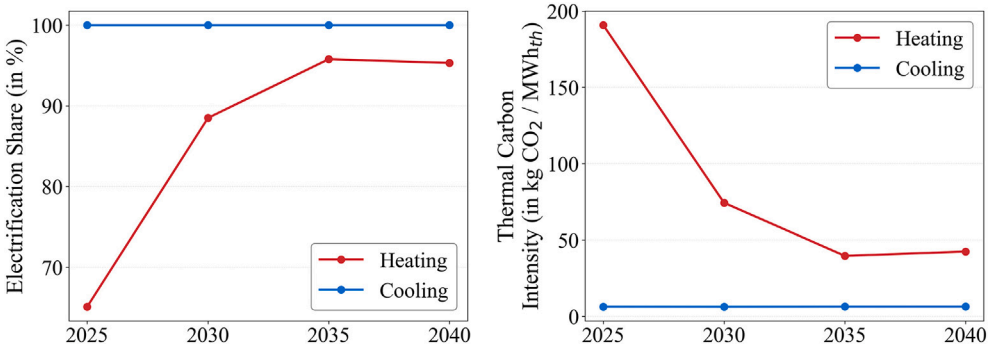

Fig. 6. Temporal evolution of system performance indicators for the base scenario (2025–2040). The left panel shows the electrification share (ES), while the right panel presents the thermal carbon intensity (TCI). Red and blue lines indicate heating- and cooling-specific values, respectively.

Data availability

Data will be made available on request.

References

[1] Wiser RH, Mills AD, Seel J, Levin T, Botterud A. Impacts of variable renewable energy on bulk power system assets, pricing, and costs. Technical Report LBNL-2001082, Lawrence Berkeley National Laboratoy; Nov 2017. https://escholarship.org/uc/item/4d01m8vt.

[2] Pereira da Silva P, Horta P. The effect of variable renewable energy sources on electricity price volatility: the case of the Iberian market. Int J Sustain Energy Sep 2019;38(8):794–813. https://doi.org/10.1080/14786451.2019.1602126. ISSN 1478-6451.

[3] Dedecca JG, Ansarin M, Bene C, van Delzen T, van Nuffel L, Jagtenberg H. Increasing flexibility in the EU energy system - technologies and policies to enable the integration of renewable electricity source. Publication for the Committee on Industry, Research and Energy, Policy Department for Transformation, Innovation and Health, Luxembourg: European Parliament; Jan 2025.

[4] Salpakari J, Mikkola J, Lund PD. Improved flexibility with large-scale variable renewable power in cities through optimal demand side management and power-to-heat conversion. Energy Convers Manag Oct 2016;126:649–61. https://doi.org/10.1016/j.enconman.2016.08.041. ISSN 01968904. https://linkinghub.elsevier.com/retrieve/pii/S0196890416307154.

[5] Golmohamadi H, Larsen KG, Jensen PG, Hasrat IR. Integration of flexibility potentials of district heating systems into electricity markets: a review. Renew Sustain Energy Rev May 2022;159:112200. https://doi.org/10.1016/j.rser.2022.112200. ISSN 13640321. https://linkinghub.elsevier.com/retrieve/pii/S136403212200123X.

[6] Ma Z, Knotzer A, Billanes JD, Jørgensen BN. A literature review of energy flexibility in district heating with a survey of the stakeholders' participation. Renew Sustain Energy Rev May 2020;123:109750. https://doi.org/10.1016/j.rser.2020.109750. ISSN 13640321. https://linkinghub.elsevier.com/retrieve/pii/S1364032120300460.

[7] Colmenar-Santos A, Rosales-Asensio E, Borge-Diez D, Mur-Pérez F. Cogeneration and district heating networks: measures to remove institutional and financial barriers that restrict their joint use in the EU-28. Energy Jun 2015;85:403–14. https://doi.org/10.1016/j.energy.2015.03.088. ISSN 03605442. https://linkinghub.elsevier.com/retrieve/pii/S0360544215003977.

[8] Billerbeck A, Breitschopf B, Winkler J, Bürger V, Köhler B, Bacquet A, Popovski E, Fallahnejad M, Kranzl L, Ragwitz M. Policy frameworks for district heating: a comprehensive overview and analysis of regulations and support measures across Europe. Energy Policy Feb 2023;173:113377. https://doi.org/10.1016/j.enpol.2022.113377. ISSN 03014215. https://linkinghub.elsevier.com/retrieve/pii/S0301421522005961.

[9] Kauko H, Delgado BM, Backe S, Sartori I. Reducing electricity demand and enhancing heat supply flexibility through energy efficiency and district heating. Energy May 2025;322:135310. https://doi.org/10.1016/j.energy.2025.135310. ISSN 03605442. https://linkinghub.elsevier.com/retrieve/pii/S0360544225009521.

[10] Luc KM, Heller A, Rode C. Energy demand flexibility in buildings and district heating systems – a literature review. Adv Build Energy Res Jul 2019;13(2):241–63. https://doi.org/10.1080/17512549.2018.1488615. ISSN 1751-2549.

[11] Bloess A, Schill W-P, Zerrahn A. Power-to-heat for renewable energy integration: a review of technologies, modeling approaches, and flexibility potentials. Appl Energy Feb 2018;212:1611–26. https://doi.org/10.1016/j.apenergy.2017.12.073. ISSN 03062619. https://linkinghub.elsevier.com/retrieve/pii/S0306261917317889.

[12] Blaauwbroek N, Nguyen PH, Konsman MJ, Shi H, Kamphuis RIG, Kling WL. Decentralized resource allocation and load scheduling for multicommodity smart energy systems. IEEE Trans Sustain Energy Oct 2015;6(4):1506–14. https://doi.org/10.1109/TSTE.2015.2441107. ISSN 1949-3029, 1949-3037. http://ieeexplore.ieee.org/document/7173437/.

[13] Parisio A, Wiezorek C, Kyntaja T, Elo J, Strunz K, Johansson KH. Cooperative MPC-based energy management for networked microgrids. IEEE Trans Smart Grid Nov 2017;8(6):3066–74. https://doi.org/10.1109/TSG.2017.2726941. ISSN 1949-3053, 1949-3061. http://ieeexplore.ieee.org/document/8004502/.

[14] Lund H, Möller B, Mathiesen BV, Dyrelund A. The role of district heating in future renewable energy systems. Energy Mar 2010;35(3):1381–90. https://doi.org/10.1016/j.energy.2009.11.023. ISSN 03605442. https://linkinghub.elsevier.com/retrieve/pii/S036054420900512X.

[15] Münster M, Morthorst PE, Larsen HV, Bregnbæk L, Werling J, Lindboe HH, Ravn H. The role of district heating in the future danish energy system. Energy Dec 2012;48(1):47–55. https://doi.org/10.1016/j.energy.2012.06.011. ISSN 03605442. https://linkinghub.elsevier.com/retrieve/pii/S0360544212004628.

[16] Askeland K, Bozhkova KN, Sorknæs P. Balancing europe: can district heating affect the flexibility potential of Norwegian hydropower resources? Renew Energy Oct 2019;141:646–56. https://doi.org/10.1016/j.renene.2019.03.137. ISSN 09601481. https://linkinghub.elsevier.com/retrieve/pii/S0960148119304586.

[17] Baldvinsson I, Nakata T. A feasibility and performance assessment of a low temperature district heating system – a north Japanese case study. Energy Jan 2016;95:155–74. https://doi.org/10.1016/j.energy.2015.11.057. ISSN 03605442. https://linkinghub.elsevier.com/retrieve/pii/S0360544215016205.

[18] Badami M, Gerboni R, Portoraro A. Determination and assessment of indices for the energy performance of district heating with cogeneration plants. Energy May 2017;127:697–703. https://doi.org/10.1016/j.energy.2017.03.136. ISSN 03605442. https://linkinghub.elsevier.com/retrieve/pii/S0360544217305297.

[19] Ferla G, Caputo P. Biomass district heating system in Italy: a comprehensive model-based method for the assessment of energy, economic and environmental performance. Energy Apr 2022;244:123105. https://doi.org/10.1016/j.energy.2022.123105. ISSN 03605442. https://linkinghub.elsevier.com/retrieve/pii/S0360544222000081.

[20] Ivancic A, Romaní J, Salom J, Cambronero M-V. Performance assessment of district energy systems with common elements for heating and cooling. Energies Apr 2021;14(8):2334. https://doi.org/10.3390/en14082334. ISSN 1996-1073. https://www.mdpi.com/1996-1073/14/8/2334.

[21] Millar M-A, Yu Z, Burnside N, Jones G, Elrick B. Identification of key performance indicators and complimentary load profiles for 5th generation district energy networks. Appl Energy Jun 2021;291:116672. https://doi.org/10.1016/j.apenergy.2021.116672. ISSN 03062619. https://linkinghub.elsevier.com/retrieve/pii/S0306261921002014.

[22] Gjoka K, Rismanchi B, Crawford RH. Towards sustainable urban energy solutions: a multi-dimensional assessment framework for fifth-generation district heating and cooling systems. Energy Build Jan 2025;326:115071. https://doi.org/10.1016/j.enbuild.2024.115071. ISSN 03787788. https://linkinghub.elsevier.com/retrieve/pii/S0378778824011873.

[23] Zhang Y, Johansson P, Sasic Kalagasidis A. Assessment of district heating and cooling systems transition with respect to future changes in demand profiles and renewable energy supplies. Energy Convers Manag Sep 2022;268:116038. https://doi.org/10.1016/j.enconman.2022.116038. ISSN 01968904. https://linkinghub.elsevier.com/retrieve/pii/S0196890422008287.

[24] Guelpa E, Verda V. Thermal energy storage in district heating and cooling systems: a review. Appl Energy Oct 2019;252:113474. https://doi.org/10.1016/j.apenergy.2019.113474. ISSN 03062619. https://linkinghub.elsevier.com/retrieve/pii/S0306261919311481.

[25] Du H, Zhou X, Nord N, Carden Y, Cui P, Ma Z. A new framework for evaluating and enhancing the performance of district heating systems integrated with data centres using short-term thermal energy storage. Energy Mar 2025;319:134934. https://doi.org/10.1016/j.energy.2025.134934. ISSN 0360-5442. https://www.sciencedirect.com/science/article/pii/S0360544225005766.

[26] Kondziella H, Bruckner T. Flexibility requirements of renewable energy based electricity systems – a review of research results and methodologies. Renew Sustain Energy Rev Jan 2016;53:10–22. https://doi.org/10.1016/j.rser.2015.07.199. ISSN 13640321. https://linkinghub.elsevier.com/retrieve/pii/S1364032115008643.

[27] Lund PD, Lindgren J, Mikkola J, Salpakari J. Review of energy system flexibility measures to enable high levels of variable renewable electricity. Renew Sustain Energy Rev May 2015;45:785–807. https://doi.org/10.1016/j.rser.2015.01.057. ISSN 13640321. https://linkinghub.elsevier.com/retrieve/pii/S1364032115000672.

[28] Degefa MZ, Sperstad IB, Sæle H. Comprehensive classifications and characterizations of power system flexibility resources. Electr Power Syst Res 2021;194:107022. https://doi.org/10.1016/j.epsr.2021.107022. ISSN 0378-7796. https://www.sciencedirect.com/science/article/pii/S037877962100002X.

[29] Alizadeh MI, Parsa Moghaddam M, Amjady N, Siano P, Sheikh-El-Eslami MK. Flexibility in future power systems with high renewable penetration: a review. Renew Sustain Energy Rev May 2016;57:1186–93. https://doi.org/10.1016/j.rser.2015.12.200. ISSN 13640321. https://linkinghub.elsevier.com/retrieve/pii/S136403211501583X.

[30] Crespo del Granado P, Rajasekharan J, Venkatesh Pandiyan S, Tomasgard A, Kara G, Farahmand H, Jaehnert S. Flexibility characterization, aggregation, and market design trends with a high share of renewables: a review. Curr Sustain/renew Energy Rep Feb 2023;10:12–21. https://doi.org/10.1007/s40518-022-00205-y

[31] Lannoye E, Flynn D, O'Malley M. Evaluation of power system flexibility. IEEE Trans Power Syst Jun 2012;27(2). https://doi.org/10.1109/TPWRS.2011.2177280

[32] Abdin AF, Zio E. An integrated framework for operational flexibility assessment in multi-period power system planning with renewable energy production. Appl Energy Jul 2018;222:898–914. https://doi.org/10.1016/j.apenergy.2018.04.009. ISSN 03062619. https://linkinghub.elsevier.com/retrieve/pii/S0306261918305518.

[33] Papaefthymiou G, Haesen E, Sach T. Power system flexibility tracker: indicators to track flexibility progress towards high-RES systems. Renew Energy Nov 2018;127:1026–35. https://doi.org/10.1016/j.renene.2018.04.094. ISSN 09601481. https://linkinghub.elsevier.com/retrieve/pii/S0960148118305196.

[34] Heggarty T, Bourmaud J-Y, Girard R, Kariniotakis G. Quantifying power system flexibility provision. Appl Energy Dec 2020;279:115852. https://doi.org/10.1016/j.apenergy.2020.115852. ISSN 03062619. https://linkinghub.elsevier.com/retrieve/pii/S030626192031326X.

[35] Li H, Wang Z, Hong T, Piette MA. Energy flexibility of residential buildings: a systematic review of characterization and quantification methods and applications. Adv Appl Energy Aug 2021;3:100054. https://doi.org/10.1016/j.adapen.2021.100054. ISSN 26667924. https://linkinghub.elsevier.com/retrieve/pii/S2666792421000469.

[36] Tang H, Wang S, Li H. Flexibility categorization, sources, capabilities and technologies for energy-flexible and grid-responsive buildings: state-of-the-art and future perspective. Energy Mar 2021;219:119598. https://doi.org/10.1016/j.energy.2020.119598. ISSN 03605442. https://linkinghub.elsevier.com/retrieve/pii/S0360544220327055.

[37] Bampoulas A, Saffari M, Pallonetto F, Mangina E, Finn DP. A fundamental unified framework to quantify and characterise energy flexibility of residential buildings with multiple electrical and thermal energy systems. Appl Energy Jan 2021;282:116096. https://doi.org/10.1016/j.apenergy.2020.116096. ISSN 03062619. https://linkinghub.elsevier.com/retrieve/pii/S0306261920315191.

[38] Stinner S, Huchtemann K, Müller D. Quantifying the operational flexibility of building energy systems with thermal energy storages. Appl Energy 2016;181:140–54. https://doi.org/10.1016/j.apenergy.2016.08.055. ISSN 0306-2619. https://www.sciencedirect.com/science/article/pii/S0306261916311424.

[39] Tang H, Wang S. Energy flexibility quantification of grid-responsive buildings: energy flexibility index and assessment of their effectiveness for applications. Energy Apr 2021;221:119756. https://doi.org/10.1016/j.energy.2021.119756. ISSN 03605442. https://linkinghub.elsevier.com/retrieve/pii/S0360544221000050.

[40] Finck C, Li R, Kramer R, Zeiler W. Quantifying demand flexibility of power-to-heat and thermal energy storage in the control of building heating systems. Appl Energy Jan 2018;209:409–25. https://doi.org/10.1016/j.apenergy.2017.11.036. ISSN 03062619. https://linkinghub.elsevier.com/retrieve/pii/S0306261917316112.

[41] Junker RG, Azar AG, Lopes RA, Lindberg KB, Reynders G, Relan R, Madsen H. Characterizing the energy flexibility of buildings and districts. Appl Energy Sep 2018;225:175–82. https://doi.org/10.1016/j.apenergy.2018.05.037. ISSN 0306-2619. https://www.sciencedirect.com/science/article/pii/S030626191830730X.

[42] Li H, Johra H, De Andrade Pereira F, Hong T, Le Dréau J, Maturo A, Wei M, Liu Y, Saberi-Derakhtenjani A, Nagy Z, Marszal-Pomianowska A, Finn D, Miyata S, Kaspar K, Nweye K, O'Neill Z, Pallonetto F, Dong B. Data-driven key performance indicators and datasets for building energy flexibility: a review and perspectives. Appl Energy Aug 2023;343:121217. https://doi.org/10.1016/j.apenergy.2023.121217. ISSN 03062619. https://linkinghub.elsevier.com/retrieve/pii/S0306261923005810.

[43] Yuan J, Zhang Y, Gang W, Tian J, Su L, Tu Z. Flexibility quantification and regulation of regional distributed energy system under multi-source uncertainties. J Clean Prod Apr 2025;501:145323. https://doi.org/10.1016/j.jclepro.2025.145323. ISSN 09596526. https://linkinghub.elsevier.com/retrieve/pii/S0959652625006730.

[44] Awan MB, Sun Y, Lin W, Ma Z. A framework to formulate and aggregate performance indicators to quantify building energy flexibility. Appl Energy Nov 2023;349:121590. https://doi.org/10.1016/j.apenergy.2023.121590. ISSN 03062619. https://linkinghub.elsevier.com/retrieve/pii/S0306261923009546.

[45] Gharibvand H, Gharehpetian GB, Anvari-Moghaddam A. A survey on microgrid flexibility resources, evaluation metrics and energy storage effects. Renew Sustain Energy Rev Sep 2024;201:114632. https://doi.org/10.1016/j.rser.2024.114632. ISSN 13640321. https://linkinghub.elsevier.com/retrieve/pii/S1364032124003587.

[46] Glücker P, Mhanna S, Pesch T, Benigni A, Mancarella P. Quantification of electrical system flexibility by local multi-energy systems: impact of the system design and component interdependencies. Appl Energy Nov 2025;397:126342. https://doi.org/10.1016/j.apenergy.2025.126342. ISSN 03062619. https://linkinghub.elsevier.com/retrieve/pii/S0306261925010724.

[47] Maitanova N, Schlüters S, Hanke B, Von Maydell K. An analytical method for quantifying the flexibility potential of decentralised energy systems. Appl Energy Jun 2024;364:123150. https://doi.org/10.1016/j.apenergy.2024.123150. ISSN 03062619. https://linkinghub.elsevier.com/retrieve/pii/S0306261924005336.

[48] Yifan Z, Wei H, Le Z, Yong M, Lei C, Zongxiang L, Ling D. Power and energy flexibility of district heating system and its application in wide-area power and heat dispatch. Energy Jan 2020;190:116426. https://doi.org/10.1016/j.energy.2019.116426. ISSN 03605442. https://linkinghub.elsevier.com/retrieve/pii/S0360544219321218.

[49] Nuytten T, Claessens B, Paredis K, Van Bael J, Six D. Flexibility of a combined heat and power system with thermal energy storage for district heating. Appl Energy Apr 2013;104:583–91. https://doi.org/10.1016/j.apenergy.2012.11.029. ISSN 03062619. https://linkinghub.elsevier.com/retrieve/pii/S0306261912008227.

[50] Guelpa E, Verda V. Demand response and other demand side management techniques for district heating: a review. Energy Mar 2021;219:119440. https://doi.org/10.1016/j.energy.2020.119440. ISSN 03605442. https://linkinghub.elsevier.com/retrieve/pii/S0360544220325470.

[51] Vandermeulen A, Van Der Heijde B, Helsen L. Controlling district heating and cooling networks to unlock flexibility: a review. Energy May 2018;151:103–15. https://doi.org/10.1016/j.energy.2018.03.034. ISSN 03605442. https://linkinghub.elsevier.com/retrieve/pii/S0360544218304328.

[52] Mitridati L, Taylor JA. Power systems flexibility from district heating networks. In: 2018 power systems computation conference (PSCC). Dublin, Ireland: IEEE; Jun 2018. p. 1–7. https://doi.org/10.23919/PSCC.2018.8442617. ISBN 978-1-910963-10-4. https://ieeexplore.ieee.org/document/8442617/.

[53] Luc KM, Li R, Xu L, Nielsen TR, Hensen JLM. Energy flexibility potential of a small district connected to a district heating system. Energy Build Oct 2020;225:110074. https://doi.org/10.1016/j.enbuild.2020.110074. ISSN 03787788. https://linkinghub.elsevier.com/retrieve/pii/S0378778819335595.

[54] Fernqvist N, Broberg S, Torén J, Svensson I-L. District heating as a flexibility service: challenges in sector coupling for increased solar and wind power production in Sweden. Energy Policy Jan 2023;172:113332. https://doi.org/10.1016/j.enpol.2022.113332. ISSN 03014215. https://linkinghub.elsevier.com/retrieve/pii/S0301421522005511.

[55] Lu F, Yu Z, Zou Y, Yang X. Cooling system energy flexibility of a nearly zero-energy office building using building thermal mass: potential evaluation and parametric analysis. Energy Build Apr 2021;236:110763. https://doi.org/10.1016/j.enbuild.2021.110763. ISSN 03787788. https://linkinghub.elsevier.com/retrieve/pii/S0378778821000475.

[56] Yin R, Kara EC, Li Y, DeForest N, Wang K, Yong T, Stadler M. Quantifying flexibility of commercial and residential loads for demand response using setpoint changes. Appl Energy Sep 2016;177:149–64. https://doi.org/10.1016/j.apenergy.2016.05.090. ISSN 03062619. https://linkinghub.elsevier.com/retrieve/pii/S0306261916306870.

[57] Zwickl-Bernhard S, Long N, Jordan S, Bauer F, Simpson JG, Trainor-Guitton W. Optimizing district energy systems under uncertainty: insights from a case study from Washington D.C. USA. Energy Convers Manag Oct 2025;341:119979. https://doi.org/10.1016/j.enconman.2025.119979. ISSN 01968904. https://linkinghub.elsevier.com/retrieve/pii/S0196890425005035.

[58] Finck C, Li R, Zeiler W. Optimal control of demand flexibility under real-time pricing for heating systems in buildings: a real-life demonstration. Appl Energy Apr 2020;263:114671. https://doi.org/10.1016/j.apenergy.2020.114671. ISSN 03062619. https://linkinghub.elsevier.com/retrieve/pii/S0306261920301835.

[59] Hirmiz R, Teamah HM, Lightstone MF, Cotton JS. Performance of heat pump integrated phase change material thermal storage for electric load shifting in building demand side management. Energy Build May 2019;190:103–18. https://doi.org/10.1016/j.enbuild.2019.02.026. ISSN 03787788. https://linkinghub.elsevier.com/retrieve/pii/S0378778818333115.

[60] Popovski E, Fleiter T, Santos H, Leal V, Fernandes EO. Technical and economic feasibility of sustainable heating and cooling supply options in Southern European municipalities-a case study for Matosinhos, Portugal. Energy Jun 2018;153:311–23. https://doi.org/10.1016/j.energy.2018.04.036. ISSN 03605442. https://linkinghub.elsevier.com/retrieve/pii/S0360544218306406.

[61] Löffler K, Hainsch K, Burandt T, Oei P-Y, Kemfert C, Von Hirschhausen C. Designing a model for the global energy system—GENeSYS-MOD: an application of the Open-Source energy modeling system (OSeMOSYS). Energies Sep 2017;10(10):1468. https://doi.org/10.3390/en10101468. ISSN 1996-1073. https://www.mdpi.com/1996-1073/10/10/1468.

[62] Löffler K. Tools to accelerate the global energy transition: assessing and improving open energy system modelling frameworks [Ph.D. thesis]. Berlin: Technische Universität Berlin; 2025.

[63] GENeSYS-MOD. The global energy system model (GENeSYS-MOD); 2024. https://github.com/GENeSYS-MOD.

[64] GENeSYS-MOD. GENeSYS-MOD documentation; 2025. https://genesysmod.readthedocs.io/en/latest/index.html#.

[65] Barani M, Löffler K, Crespo Del Granado P, Moskalenko N, Panos E, Hoffart FM, Hirschhausen von C, Kannavou M, Auer H, Hainsch K, González Grandón T, Mathisen S, Tomasgard A. European energy vision 2050 and beyond: designing scenarios for europe's energy transition. Renew Sustain Energy Rev Jan 2026;225:116074. https://doi.org/10.1016/j.rser.2025.116074. ISSN 13640321. https://linkinghub.elsevier.com/retrieve/pii/S1364032125007476.

[66] Jordan S. District thermal energy systems with power markets; Oct 2025. https://github.com/SimonJordan/district_thermal_energy_systems_with_power_markets. original-date: 2024-06-05T08:44:40Z.

[67] Heimar Andersen K, Krekling Lien S, Byskov Lindberg K, Taxt Walnum H, Sartori I. Further development and validation of the "PROFet" energy demand load profiles estimator; Sep 2021. https://doi.org/10.26868/25222708.2021.30159. https://publications.ibpsa.org/conference/paper/?id=bs2021_30159.

[68] European Parliament. What progress has the EU made against climate change? (Infographics); Jul 2018. https://www.europarl.europa.eu/topics/en/article/20180706STO07407/what-progress-has-the-eu-made-against-climate-change-infographics.

[69] Kauko H, Brækken A, Askeland M. Flexibility through power-to-heat in local integrated energy systems with renewable electricity generation and seasonal thermal energy storage. Energy Dec 2024;313:134017. https://doi.org/10.1016/j.energy.2024.134017. ISSN 03605442. https://linkinghub.elsevier.com/retrieve/pii/S0360544224037952.

[70] Vilén K, Ahlgren EO. Seasonal large-scale thermal energy storage in an evolving district heating system – long-term modeling of interconnected supply and demand. Smart Energy Aug 2024;15:100156. https://doi.org/10.1016/j.segy.2024.100156. ISSN 26669552. https://linkinghub.elsevier.com/retrieve/pii/S2666955224000261.

[71] Kauko H, Pinel D, Graabak I, Wolfgang O. Assessing the potential of seasonal thermal storage for local energy systems: case study for a neighborhood in Norway. Smart Energy May 2022;6:100075. https://doi.org/10.1016/j.segy.2022.100075. ISSN 26669552. https://linkinghub.elsevier.com/retrieve/pii/S2666955222000132.

[72] Jebamalai JM, Marlein K, Laverge J. Influence of centralized and distributed thermal energy storage on district heating network design. Energy Jul 2020;202:117689. https://doi.org/10.1016/j.energy.2020.117689. ISSN 03605442. https://linkinghub.elsevier.com/retrieve/pii/S0360544220307969.

[73] Mäki E, Kannari L, Hannula I, Shemeikka J. Decarbonization of a district heating system with a combination of solar heat and bioenergy: a techno-economic case study in the Northern European context. Renew Energy Sep 2021;175:1174–99. https://doi.org/10.1016/j.renene.2021.04.116. ISSN 09601481. https://linkinghub.elsevier.com/retrieve/pii/S0960148121006364.

[74] Sandberg E, Sneum DM, Trømborg E. Framework conditions for nordic district heating - similarities and differences, and why Norway sticks out. Energy Apr 2018;149:105–19. https://doi.org/10.1016/j.energy.2018.01.148. ISSN 03605442. https://linkinghub.elsevier.com/retrieve/pii/S0360544218301762.

[75] Tian Z, Zhang S, Deng J, Fan J, Huang J, Kong W, Perers B, Furbo S. Large-scale solar district heating plants in Danish smart thermal grid: developments and recent trends. Energy Convers Manag Jun 2019;189:67–80. https://doi.org/10.1016/j.enconman.2019.03.071. ISSN 01968904. https://linkinghub.elsevier.com/retrieve/pii/S0196890419303759.

[76] Hirvonen J, Kosonen R. Waste incineration heat and seasonal thermal energy storage for promoting economically optimal Net-Zero energy districts in Finland. Buildings Nov 2020;10(11):205. https://doi.org/10.3390/buildings10110205. ISSN 2075-5309. https://www.mdpi.com/2075-5309/10/11/205.

[77] Sukumaran S, Pugal SE, Ofili S, Kirs T, Rabani MB, Volkova A. Multi-Parametric analysis of a district cooling system integrated with energy storage technologies: a case study of a university campus in Northern Europe. Environ Clim Technol Jan 2025;29(1):512–26. https://doi.org/10.2478/rtuect-2025-0035. ISSN 2255-8837. https://www.sciendo.com/article/10.2478/rtuect-2025-0035.

[78] Cowley T, Hutty T, Hammond J, Brown S. Achieving emission reduction through the utilisation of local low-grade heat sources in district heating networks. Appl Therm Eng Apr 2024;242:122381. https://doi.org/10.1016/j.applthermaleng.2024.122381. ISSN 13594311. https://linkinghub.elsevier.com/retrieve/pii/S1359431124000498.

[79] Malcher X, Gonzalez-Salazar M. Strategies for decarbonizing european district heating: evaluation of their effectiveness in Sweden, France, Germany, and Poland. Energy Oct 2024;306:132457. https://doi.org/10.1016/j.energy.2024.132457. ISSN 03605442. https://linkinghub.elsevier.com/retrieve/pii/S036054422402231X.

[80] Brunak K, Kofoed-Wiuff A, Lindroos T, Bozhkova K. Tracking nordic clean energy progress 2025. Nordic Energy Research; 2025. https://doi.org/10.6027/NER2024-05. https://pub.norden.org/nordicenergyresearch2024-05/.

[81] Testasecca T, Catrini P, La Villetta M, Beccali M, Piacentino A. Energy assessment of thermal solar-powered district heating and cooling networks for a cluster of buildings in Mediterranean climate. Renew Energy Oct 2025;251:123397. https://doi.org/10.1016/j.renene.2025.123397. ISSN 09601481. https://linkinghub.elsevier.com/retrieve/pii/S0960148125010596.

[82] European Commission. Joint Research Centre. Efficient district heating and cooling systems in the EU: case studies analysis, replicable key success factors and potential policy implications. LU: Publications Office; 2016. https://data.europa.eu/doi/10.2760/371045.

[83] Bertelsen N, Mathiesen BV. EU-28 residential heat supply and consumption: historical development and status. Energies Apr 2020;13(8):1894. https://doi.org/10.3390/en13081894. ISSN 1996-1073. https://www.mdpi.com/1996-1073/13/8/1894.

[84] Slorach PC, Stamford L. Net zero in the heating sector: technological options and environmental sustainability from now to 2050. Energy Convers Manag Feb 2021;230:113838. https://doi.org/10.1016/j.enconman.2021.113838. ISSN 01968904. https://linkinghub.elsevier.com/retrieve/pii/S0196890421000157.

[85] Unegg MC, Steininger KW, Ramsauer C, Rivera-Aguilar M. Assessing the environmental impact of waste management: a comparative study of CO_2 emissions with a focus on recycling and incineration. J Clean Prod Aug 2023;415:137745. https://doi.org/10.1016/j.jclepro.2023.137745. ISSN 09596526. https://linkinghub.elsevier.com/retrieve/pii/S0959652623019030.

[86] The Norwegian Energy Regulatory Authority (RME). Electricity disclosure 2018 - NVE; 2021. https://www.nve.no/norwegian-energy-regulatory-authority/retail-market/electricity-disclosure-2018/.